SIAM J. NUMER. ANAL.
Vol. 56, No. 3, pp. 1210–1242

VIRTUAL ELEMENTS FOR THE NAVIER–STOKES PROBLEM ON POLYGONAL MESHES*

L. BEIRÃO DA VEIGA†, C. LOVADINA‡, AND G. VACCA†

Abstract. A family of virtual element methods for the two-dimensional Navier–Stokes equations is proposed and analyzed. The schemes provide a discrete velocity field which is pointwise divergence-free. A rigorous error analysis is developed, showing that the methods are stable and optimally convergent. Several numerical tests are presented, confirming the theoretical predictions. A comparison with some mixed finite elements is also performed.

Key words. virtual element method, polygonal meshes, Navier–Stokes equations

AMS subject classifications. 65N30, 76D05

DOI. 10.1137/17M1132811

1. Introduction.

The virtual element method (VEM), introduced in [11, 12], is a recent paradigm for the approximation of partial differential equation problems that shares the same variational background as the finite element methods. The original motivation of VEM is the need to construct an accurate *conforming* Galerkin scheme with the capability to deal with highly general polygonal/polyhedral meshes, including "hanging vertexes" and nonconvex shapes. Among the Galerkin schemes, VEM is peculiar in that the discrete spaces consist of functions which are not known pointwise, but about which a limited set of information is available. This limited information is sufficient to construct the stiffness matrix and the right-hand side.

The VEM has been developed for many problems; see, for example, [23, 1, 10, 43, 46, 9, 19, 17, 18, 6, 42, 54, 51, 37, 45]. More specifically, with regard to the Stokes problem, virtual elements have been developed in [3, 28, 15, 25, 26, 52]. Moreover, VEM is also attracting growing interest for continuum mechanics problems within the engineering community. We cite here the recent works [36, 13, 4, 53, 30, 2, 35] and [8, 24, 5], for instance. Finally, some examples of other numerical methods for the Stokes or Navier–Stokes equations that can handle polytopal meshes are [33, 47, 32].

In this paper, we initiate the development of the VEM for the Navier–Stokes equations. We limit the study to *two-dimensional domains* and to *diffusion dominated* cases. Although this is the simplest situation, it is nonetheless challenging and shows the satisfactory performance of the method; considering more complex cases will be a further step in future work. The presented scheme may be considered as a natural evolution of our recent divergence-free approach developed in [15] for the Stokes problem. However, the nonlinear convective term in the Navier–Stokes equations leads to the introduction of suitable projectors. These, in turn, suggest making use of an enhanced discrete velocity space [52], which is an improvement with respect

*Received by the editors June 5, 2017; accepted for publication (in revised form) February 5, 2018; published electronically May 1, 2018.

http://www.siam.org/journals/sinum/56-3/M113281.html

Funding: The work of the first and third authors was partially supported by the European Research Council through the H2020 Consolidator Grant (grant 681162) CAVE, Challenges and Advancements in Virtual Elements. This support is gratefully acknowledged.

†Dipartimento di Matematica e Applicazioni, Università degli Studi di Milano Bicocca, 20125 Milano, Italy (lourenco.beirao@unimib.it, giuseppe.vacca@unimib.it).

‡Dipartimento di Matematica, Università degli Studi di Milano, 20133 Milano, Italy (carlo.lovadina@unimi.it).

to that of [15]. Instead, the pressure field is approximated by means of standard locally polynomial functions, without any continuity requirement across the elements. Furthermore, we consider two different discretizations of the trilinear form arising from the convective term.

The first is the straightforward VEM version of the continuous trilinear form; however, the projector introduction causes a lack of skew-symmetry, even though the discrete velocity is divergence-free (up to machine precision). This leads us to consider the second choice, which is simply the skew-symmetric part of the trilinear form mentioned above (cf., for instance, [38] and, in the VEM framework, [29]). We remark that we develop an error analysis focusing on this latter choice, but the numerical tests concern both alternatives. The outcome is a family of virtual elements, one per each polynomial order of consistency k, with $k \geq 2$. To the best of our knowledge, this is the first paper where the VEM technology is applied to the Navier–Stokes equations.

The main objectives of the present paper are the following:

- *The development of a rigorous error analysis of the proposed methods.* We highlight that our analysis provides some noteworthy element of novelty. Indeed, although we follow rather well-established lines for the error analysis of two-dimensional Navier–Stokes Galerkin methods (see, for example, [38]), these need to be combined with new techniques that are peculiar to the VEM framework. In particular, the interpolant construction of Theorem 4.1 involves new arguments which might be useful even in different contexts (i.e., for other VEM spaces with different regularity requirements).
- *A first but thorough assessment of the actual numerical performance of this new approach.* We provide a set of numerical tests that highlight the features of our VEM approach. In addition to the important flexibility of dealing with general polygonal meshes, the presented scheme (we tested the case $k = 2$) displays the following favorable points:
  1. The error components partly decouple: notably, the velocity error does not depend directly on the discrete pressures, but only indirectly through the approximation of the loading and convection terms. This is a consequence of the fact that our methods provide a discrete velocity which is pointwise divergence-free (the isochoric constraint is *not* relaxed). In some situations, e.g., for hydrostatic fluid problems, the partial decoupling of the errors induces a positive effect on the velocity approximation. Moreover, for the same reason, the VEM scheme seems to be more robust for small values of the viscosity parameter when compared with standard mixed finite elements.
  2. Another advantage of the method is that, again due to its divergence-free nature, the same virtual space couple also can be used directly for the approximation of the diffusion problem (in mixed form). This allows for a much easier coupling in Stokes–Darcy problems where different models need to be used in different parts of the domain. This observation adds up with the fact that, thanks to the use of polygons that allow hanging nodes, the gluing of different meshes in different parts of the domain is also much easier.
  3. As in [15], the particular choice of degrees of freedom (DoFs) adopted for the velocity space yields a diagonal structure in a large part of the velocity-pressure interaction stiffness matrix. As a consequence, and without the need for any static condensation, many internal-to-element DoFs can be automatically ignored when building the linear system.

We finally note that, currently, there do exist Galerkin-type finite element methods for the Stokes and Navier–Stokes equations that are pressure-robust (that is, the error on the velocity does not depend on the pressure, not even indirectly through the loading or convection terms). Some recent examples of such schemes can be found in [40, 34], while a comprehensive review is provided in [39]. However, to the best of our knowledge, all of the available schemes work only for standard simplicial/hexahedral meshes. Although our method is not pressure-robust in the sense above, for arbitrary polygonal meshes it is the only conforming divergence-free scheme, a property which yields important advantages, as outlined in points 1 and 2. Developing a conforming scheme which is both divergence-free and pressure-robust for general polygonal meshes is currently an open problem.

A brief outline of the paper follows. In section 2 we recall the two-dimensional Navier–Stokes problem, introducing the classical variational formulation and the necessary notation. Section 3 details the proposed discretization procedure. The approximation spaces and all of the quantities that form the discrete problem are introduced and described. Section 4 deals with the theoretical analysis, which leads to the optimal error estimates of Theorem 4.6 and bound (94). Finally, section 5 presents several numerical tests which highlight the actual performance of our approach, also in comparison with a couple of well-known mixed finite element schemes.

2. The continuous Navier–Stokes equation. We consider the steady Navier–Stokes equation on a polygonal domain $\Omega \subseteq \mathbb{R}^2$ with homogeneous Dirichlet boundary conditions:

$$
(1) \qquad \begin{cases} \text{find } (\mathbf{u}, p), \text{ such that (s.t.)} & \\ -\nu\,\boldsymbol{\Delta}\mathbf{u} + (\boldsymbol{\nabla}\mathbf{u})\,\mathbf{u} - \nabla p = \mathbf{f} & \text{in } \Omega, \\ \operatorname{div}\mathbf{u} = 0 & \text{in } \Omega, \\ \mathbf{u} = 0 & \text{on } \Gamma = \partial\Omega, \end{cases}
$$

with $\nu \in \mathbb{R}$, $\nu > 0$, and where $\mathbf{u}, p$ are the velocity and the pressure fields, respectively. Furthermore, $\boldsymbol{\Delta}$, div, $\boldsymbol{\nabla}$, and ∇ denote the vector Laplacian, the divergence, the gradient operator for vector fields, and the gradient operator for scalar functions. Finally, $\mathbf{f}$ represents the external force, while ν is the viscosity. We also remark that different boundary conditions can be treated as well.

Let us consider the spaces

$$
(2) \qquad \mathbf{V} := \left[H_0^1(\Omega)\right]^2, \qquad Q := L_0^2(\Omega) = \left\{ q \in L^2(\Omega) \quad \text{s.t.} \quad \int_\Omega q \,\mathrm{d}\Omega = 0 \right\}
$$

with norms

$$
(3) \qquad \|\mathbf{v}\|_{\mathbf{V}} := |\mathbf{v}|_{[H^1(\Omega)]^2}, \qquad \|q\|_Q := \|q\|_{L^2(\Omega)}.
$$

We assume $\mathbf{f} \in [L^2(\Omega)]^2$ and consider the linear forms

$$
(4) \qquad a(\cdot,\cdot)\colon \mathbf{V}\times\mathbf{V} \to \mathbb{R}, \qquad a(\mathbf{u},\mathbf{v}) := \int_\Omega \boldsymbol{\nabla}\mathbf{u} : \boldsymbol{\nabla}\mathbf{v} \,\mathrm{d}\Omega \qquad \text{for all } \mathbf{u},\mathbf{v} \in \mathbf{V},
$$

$$
(5) \qquad b(\cdot,\cdot)\colon \mathbf{V}\times Q \to \mathbb{R}, \qquad b(\mathbf{v},q) := \int_\Omega q \operatorname{div}\mathbf{v} \,\mathrm{d}\Omega \qquad \text{for all } \mathbf{v} \in \mathbf{V},\ q \in Q,
$$

$$
(6) \qquad c(\cdot;\,\cdot,\cdot)\colon \mathbf{V}\times\mathbf{V}\times\mathbf{V} \to \mathbb{R}, \qquad c(\mathbf{w};\,\mathbf{u},\mathbf{v}) := \int_\Omega (\boldsymbol{\nabla}\mathbf{u})\,\mathbf{w}\cdot\mathbf{v} \,\mathrm{d}\Omega \qquad \text{for all } \mathbf{w},\mathbf{u},\mathbf{v} \in \mathbf{V}.
$$

Then a standard variational formulation of problem (1) is

$$\begin{cases} \text{find } (\mathbf{u},p)\in \mathbf{V}\times Q, \text{ s.t.} \\ \nu\, a(\mathbf{u},\mathbf{v}) + c(\mathbf{u};\,\mathbf{u},\mathbf{v}) + b(\mathbf{v},p) = (\mathbf{f},\mathbf{v}) & \text{for all } \mathbf{v}\in\mathbf{V}, \\ b(\mathbf{u},q) = 0 & \text{for all } q\in Q, \end{cases} \tag{7}$$

where

$$(\mathbf{f},\mathbf{v}) := \int_\Omega \mathbf{f}\cdot\mathbf{v}\,\mathrm{d}\Omega.$$

It is well known that with the choices (3), we have (see, for instance, [38]) the following:

- $a(\cdot,\cdot)$, $b(\cdot,\cdot)$, and $c(\cdot;\,\cdot,\cdot)$ are continuous, i.e.,

$$\begin{aligned} |a(\mathbf{u},\mathbf{v})| &\le \|\mathbf{u}\|_{\mathbf{V}}\|\mathbf{v}\|_{\mathbf{V}} && \text{for all } \mathbf{u},\mathbf{v}\in\mathbf{V}, \\ |b(\mathbf{v},q)| &\le \|\mathbf{v}\|_{\mathbf{V}}\|q\|_Q && \text{for all } \mathbf{v}\in\mathbf{V} \text{ and } q\in Q, \\ |c(\mathbf{w};\,\mathbf{u},\mathbf{v})| &\le \widehat{C}\,\|\mathbf{w}\|_{\mathbf{V}}\|\mathbf{u}\|_{\mathbf{V}}\|\mathbf{v}\|_{\mathbf{V}} && \text{for all } \mathbf{w},\mathbf{u},\mathbf{v}\in\mathbf{V}. \end{aligned}$$

- $a(\cdot,\cdot)$ is coercive (with coercivity constant $\alpha = 1$), i.e.,

$$a(\mathbf{v},\mathbf{v}) \ge \|\mathbf{v}\|^2_{\mathbf{V}} \qquad \text{for all } \mathbf{v}\in\mathbf{V}.$$

- The bilinear form $b(\cdot,\cdot)$ and the space $\mathbf{V}$ and Q satisfy the inf-sup condition, i.e.,

$$\exists\,\beta>0 \quad \text{s.t.} \quad \sup_{\mathbf{v}\in\mathbf{V},\,\mathbf{v}\neq\mathbf{0}} \frac{b(\mathbf{v},q)}{\|\mathbf{v}\|_{\mathbf{V}}} \ge \beta\|q\|_Q \qquad \text{for all } q\in Q. \tag{8}$$

Therefore, if

$$\gamma := \frac{\widehat{C}\,\|\mathbf{f}\|_{-1}}{\nu^2} < 1, \tag{9}$$

then problem (7) has a unique solution $(\mathbf{u},p)\in\mathbf{V}\times Q$ such that

$$\|\mathbf{u}\|_{\mathbf{V}} \le \frac{\|\mathbf{f}\|_{H^{-1}}}{\nu}. \tag{10}$$

Let us introduce the kernel

$$\mathbf{Z} := \{\mathbf{v}\in\mathbf{V} \quad \text{s.t.} \quad b(\mathbf{v},q) = 0 \quad \text{for all } q\in Q\}. \tag{11}$$

Then problem (7) can be formulated in the equivalent kernel form

$$\begin{cases} \text{find } \mathbf{u}\in\mathbf{Z}, \text{ s.t.} \\ \nu\, a(\mathbf{u},\mathbf{v}) + c(\mathbf{u};\,\mathbf{u},\mathbf{v}) = (\mathbf{f},\mathbf{v}) & \text{for all } \mathbf{v}\in\mathbf{Z}. \end{cases} \tag{12}$$

Finally, by a direct computation it is easy to see that if $\mathbf{u}\in\mathbf{Z}$ is fixed, then the bilinear form $c(\mathbf{u};\,\cdot,\,\cdot)\colon \mathbf{V}\times\mathbf{V}\to\mathbb{R}$ is skew-symmetric, i.e.,

$$c(\mathbf{u};\mathbf{v},\mathbf{w}) = -c(\mathbf{u};\mathbf{w},\mathbf{v}) \qquad \text{for all } \mathbf{v},\mathbf{w}\in\mathbf{V}.$$

Therefore we introduce, as usual, also the trilinear form $\widetilde{c}(\cdot,\,\cdot,\,\cdot)\colon \mathbf{V}\times\mathbf{V}\times\mathbf{V}\to\mathbb{R}$:

$$\widetilde{c}(\mathbf{w};\,\mathbf{u},\mathbf{v}) := \frac{1}{2}c(\mathbf{w};\,\mathbf{u},\mathbf{v}) - \frac{1}{2}c(\mathbf{w};\,\mathbf{v},\mathbf{u}) \qquad \text{for all } \mathbf{w},\mathbf{u},\mathbf{v}\in\mathbf{V}. \tag{13}$$

3. Virtual formulation of the problem.

3.1. Virtual element space and polynomial projections. We outline the virtual element discretization of problem (7). We will make use of various tools from the virtual element technology, which will be described briefly; we refer the interested reader to the papers [15, 52].

Let $\{\Omega_h\}_h$ be a sequence of decompositions of Ω into general polygonal elements E with

$$h_E := \text{diameter}(E), \quad h := \sup_{E\in\Omega_h} h_E.$$

We suppose that for all h, each element E in Ω_h fulfills the following assumptions:

(A1) E is star-shaped with respect to a ball B_E of radius $\geq \varrho\, h_E$.

(A2) The distance between any two vertexes of E is $\geq c\, h_E$,

where ϱ and c are positive constants. We remark that the hypotheses above, though not too restrictive in many practical cases, can be further relaxed, as investigated in [14]. Using standard VEM notation, for $k \in \mathbb{N}$, let us define the spaces

- $\mathbb{P}_k(E)$, the set of polynomials on E of degree $\leq k$ (with the extended notation $\mathbb{P}_{-1}(E) = \emptyset$),
- $\mathbb{B}_k(E) := \{v \in C^0(\partial E) \text{ s.t. } v_{|e} \in \mathbb{P}_k(e) \text{ for all edges } e \subset \partial E\}$,
- $\mathcal{G}_k(E) := \nabla(\mathbb{P}_{k+1}(E)) \subseteq [\mathbb{P}_k(E)]^2$,
- $\mathcal{G}_k^{\oplus}(E) := \mathbf{x}^{\perp}[\mathbb{P}_{k-1}(E)] \subseteq [\mathbb{P}_k(E)]^2$ with $\mathbf{x}^{\perp} := (x_2, -x_1)$.

For any $n \in \mathbb{N}$ and $E \in \Omega_h$ we introduce the following useful polynomial projections:

- the $\boldsymbol{H^1}$ **seminorm projection** $\Pi_n^{\nabla,E}\colon \mathbf{V} \to [\mathbb{P}_n(E)]^2$, defined by

$$\begin{cases} \displaystyle\int_E \boldsymbol{\nabla}\,\mathbf{q}_n : \boldsymbol{\nabla}(\mathbf{v} - \Pi_n^{\nabla,E}\mathbf{v})\,\mathrm{d}E = 0 \quad \text{for all } \mathbf{v} \in \mathbf{V} \text{ and for all } \mathbf{q}_n \in [\mathbb{P}_n(E)]^2, \\ \Pi_0^{0,E}(\mathbf{v} - \Pi_n^{\nabla,E}\mathbf{v}) = \mathbf{0}, \end{cases} \tag{14}$$

- the $\boldsymbol{L^2}$**-projection for scalar functions** $\Pi_n^{0,E}\colon L^2(E) \to \mathbb{P}_n(E)$, given by

$$\int_E q_n(v - \Pi_n^{0,E}v)\,\mathrm{d}E = 0 \qquad \text{for all } v \in L^2(E) \text{ and for all } q_n \in \mathbb{P}_n(E), \tag{15}$$

  with obvious extension for vector functions $\Pi_n^{0,E}\colon [L^2(\Omega)]^2 \to [\mathbb{P}_n(E)]^2$ and tensor functions $\boldsymbol{\Pi}_n^{0,E}\colon [L^2(E)]^{2\times 2} \to [\mathbb{P}_n(E)]^{2\times 2}$.

In [15] we have introduced a new family of virtual elements for the Stokes problem on polygonal meshes. In particular, by a proper choice of the virtual space of velocities, the virtual local spaces are associated to a Stokes-like variational problem on each element. In [52] we have presented an enhanced virtual space, taking the inspiration from [1], to be used in place of the original one in such a way that the L^2-projection can be exactly computable by the DoFs. In this section we briefly recall from [15, 52] the notation, the main properties of the virtual spaces, and some details about the construction of the projections.

Let $k \geq 2$ be the polynomial degree of accuracy of the method. We introduce on each element $E \in \Omega_h$ the (original) finite-dimensional local virtual space [15]

$$\mathbf{W}_h^E := \Bigg\{ \mathbf{v} \in [H^1(E)]^2 \quad \text{s.t.} \quad \mathbf{v}_{|\partial E} \in [\mathbb{B}_k(\partial E)]^2\,, \\ \begin{cases} -\boldsymbol{\Delta}\mathbf{v} - \nabla s \in \mathcal{G}_{k-2}^{\oplus}(E), \\ \operatorname{div}\mathbf{v} \in \mathbb{P}_{k-1}(E), \end{cases} \quad \text{for some } s \in L^2(E) \Bigg\}, \tag{16}$$

where all the operators and equations above are to be interpreted in the distributional sense. Then we enlarge the previous space

$$\mathbf{U}_h^E := \Bigg\{ \mathbf{v} \in [H^1(E)]^2 \quad \text{s.t.} \quad \mathbf{v}_{|\partial E} \in [\mathbb{B}_k(\partial E)]^2 \,, \\ \begin{cases} -\boldsymbol{\Delta}\mathbf{v} - \nabla s \in \mathcal{G}_k^{\oplus}(E), \\ \operatorname{div}\mathbf{v} \in \mathbb{P}_{k-1}(E), \end{cases} \quad \text{for some } s \in L^2(E) \Bigg\}.$$

Now we define the virtual element space $\mathbf{V}_h^E$ as the restriction of $\mathbf{U}_h^E$ given by

(17)
$$\mathbf{V}_h^E := \left\{ \mathbf{v} \in \mathbf{U}_h^E \quad \text{s.t.} \quad \left(\mathbf{v} - \Pi_k^{\nabla,E}\mathbf{v},\, \mathbf{g}_k^{\perp} \right)_{[L^2(E)]^2} = 0 \quad \text{for all } \mathbf{g}_k^{\perp} \in \mathcal{G}_k^{\oplus}(E)/\mathcal{G}_{k-2}^{\oplus}(E) \right\},$$

where the symbol $\mathcal{G}_k^{\oplus}(E)/\mathcal{G}_{k-2}^{\oplus}(E)$ denotes the polynomials in $\mathcal{G}_k^{\oplus}(E)$ that are L^2-orthogonal to all polynomials of $\mathcal{G}_{k-2}^{\oplus}(E)$ (observing that $\mathcal{G}_{k-2}^{\oplus}(E) \subset \mathcal{G}_k^{\oplus}(E)$). From [9, 15, 52], we recall the following properties of the space $\mathbf{V}_h^E$ (see [52] for the proof).

PROPOSITION 3.1 (dimension and DoFs). *Let $\mathbf{V}_h^E$ be the space defined in* (17). *Then the dimension of $\mathbf{V}_h^E$ is*

$$\begin{aligned} \dim\left(\mathbf{V}_h^E\right) &= \dim\left([\mathbb{B}_k(\partial E)]^2\right) + \dim\left(\mathcal{G}_{k-2}^{\oplus}(E)\right) + (\dim(\mathbb{P}_{k-1}(E)) - 1) \\ &= 2n_E k + \frac{(k-1)(k-2)}{2} + \frac{(k+1)k}{2} - 1, \end{aligned} \tag{18}$$

where n_E is the number of vertexes of E. Moreover, the following linear operators $\mathbf{D_V}$, split into four subsets (see Figure 1) constitute a set of DoFs for $\mathbf{V}_h^E$:

- $\mathbf{D_V 1}$: *the values of* $\mathbf{v}$ *at the vertexes of the polygon* E,
- $\mathbf{D_V 2}$: *the values of* $\mathbf{v}$ *at* $k-1$ *distinct points of every edge* $e \in \partial E$,
- $\mathbf{D_V 3}$: *the moments of* $\mathbf{v}$,

$$\int_E \mathbf{v} \cdot \mathbf{g}_{k-2}^{\oplus} \,\mathrm{d}E \qquad \textit{for all } \mathbf{g}_{k-2}^{\oplus} \in \mathcal{G}_{k-2}^{\oplus}(E),$$

- $\mathbf{D_V 4}$: *the moments of* $\operatorname{div}\mathbf{v}$,

$$\int_E (\operatorname{div}\mathbf{v})\, q_{k-1} \,\mathrm{d}E \qquad \textit{for all } q_{k-1} \in \mathbb{P}_{k-1}(E)/\mathbb{R}.$$

We highlight that the DoFs $\mathbf{D_V 1}$ and $\mathbf{D_V 2}$ are directly related to the piecewise polynomial boundary space $[\mathbb{B}_k(\partial E)]^2$, while the DoFs $\mathbf{D_V 4}$ are naturally associated to the condition $\operatorname{div}\mathbf{v} \in \mathbb{P}_{k-1}(E)$. The role of the DoFs $\mathbf{D_V 3}$ is more subtle (see [15]) and is related to the first equation in the definition of the virtual space. The proof of the following result can be found in [15] for $\Pi_{\mathrm{k}}^{\nabla,\mathrm{E}}$ and in [52] for the remaining projectors.

PROPOSITION 3.2 (projections and computability). *The DoFs $\mathbf{D_V}$ allow us to compute exactly*

$$\Pi_{\mathrm{k}}^{\nabla,\mathrm{E}} \colon \mathbf{V}_h^E \to [\mathbb{P}_k(E)]^2, \quad \Pi_{\mathrm{k}}^{0,\mathrm{E}} \colon \mathbf{V}_h^E \to [\mathbb{P}_k(E)]^2, \quad \boldsymbol{\Pi}_{\mathrm{k-1}}^{0,\mathrm{E}} \colon \boldsymbol{\nabla}(\mathbf{V}_h^E) \to [\mathbb{P}_{k-1}(E)]^{2\times 2},$$

in the sense that, given any $\mathbf{v}_h \in \mathbf{V}_h^E$, we are able to compute the polynomials $\Pi_{\mathrm{k}}^{\nabla,\mathrm{E}}\,\mathbf{v}_h$, $\Pi_{\mathrm{k}}^{0,\mathrm{E}}\,\mathbf{v}_h$, and $\boldsymbol{\Pi}_{\mathrm{k-1}}^{0,\mathrm{E}}\,\nabla\mathbf{v}_h$ using only, as unique information, the DoFs values $\mathbf{D_V}$ of $\mathbf{v}_h$.

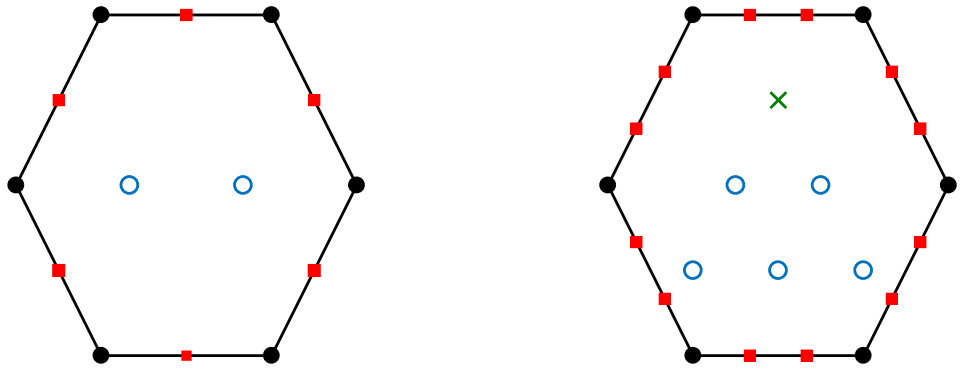

FIG. 1. *DoFs for $k = 2$, $k = 3$. We denote $\mathbf{D_V 1}$ with the dots, $\mathbf{D_V 2}$ with the squares, $\mathbf{D_V 3}$ with the crosses, and $\mathbf{D_V 4}$ with the circles.*

Remark 3.1. Using the enhanced space $\mathbf{V}_h^E$ and following along the same ideas of [15, 52], it is possible to improve the results of Proposition 3.2 and compute exactly also the following higher order projections:

$$\Pi_{k+2}^{\nabla,E}\colon \mathbf{V}_h^E \to [\mathbb{P}_{k+2}(E)]^2, \qquad \mathbf{\Pi}_{k+1}^{0,E}\colon \boldsymbol{\nabla}(\mathbf{V}_h^E) \to [\mathbb{P}_{k+1}(E)]^{2\times 2}.$$

Moreover, given any polynomial q_n of arbitrary degree n and any $\mathbf{v} \in \mathbf{V}_h^E$, an integration by parts shows that we can compute the moment

$$\int_E \nabla q_n \cdot \mathbf{v}\, \mathrm{d}E.$$

For the pressures we take the standard finite-dimensional space

$$Q_h^E := \mathbb{P}_{k-1}(E) \tag{19}$$

having dimension

$$\dim(Q_h^E) = \dim(\mathbb{P}_{k-1}(E)) = \frac{(k+1)k}{2}.$$

The corresponding DoFs are chosen, defining for each $q \in Q_h^E$ the following linear operators $\mathbf{D_Q}$:

- $\mathbf{D_Q}$: the moments up to order $k-1$ of q, i.e.,

$$\int_E q\, p_{k-1}\, \mathrm{d}E \qquad \text{for all } p_{k-1} \in \mathbb{P}_{k-1}(E).$$

Finally we define the global virtual element spaces as

$$\mathbf{V}_h := \{\mathbf{v} \in [H_0^1(\Omega)]^2 \quad \text{s.t.} \quad \mathbf{v}_{|E} \in \mathbf{V}_h^E \quad \text{for all } E \in \Omega_h\} \tag{20}$$

and

$$Q_h := \{q \in L_0^2(\Omega) \quad \text{s.t.} \quad q_{|E} \in Q_h^E \quad \text{for all } E \in \Omega_h\}, \tag{21}$$

with the obvious associated sets of global DoFs. A simple computation shows that

$$\dim(\mathbf{V}_h) = n_P \left(\frac{(k+1)k}{2} - 1 + \frac{(k-1)(k-2)}{2} \right) + 2(n_V + (k-1)n_e)$$

and

$$\dim(Q_h) = n_P \frac{(k+1)k}{2} - 1,$$

where n_P is the number of elements, and n_e and n_V are the number of internal edges and vertexes in Ω_h. As observed in [15], we remark that

$$\operatorname{div} \mathbf{V}_h \subseteq Q_h, \tag{22}$$

a key property that will lead to a *divergence-free* discrete solution.

Remark 3.2. In the survey work [39], the authors classify the divergence-free mixed finite element methods into three groups: (1) conforming schemes, (2) discontinuous Galerkin schemes, and (3) schemes with an appropriate reconstruction of the test functions.

The VEM we are proposing may fall into the first group, with the additional flexibility to be used in connection with polytopal meshes.

3.2. Discrete bilinear forms and load term approximation. The next step in the construction of our method is to define a discrete version of the bilinear forms $a(\cdot,\cdot)$ and $b(\cdot,\cdot)$ given in (4) and (5) and the trilinear form $c(\cdot;\cdot,\cdot)$ in (6). Here and in the rest of the paper the symbol C will indicate a generic positive quantity that is independent of the mesh size (and of ν), but may depend on Ω and on the polynomial degree k. Furthermore, C may vary at each occurrence. First we decompose into local contributions the bilinear forms $a(\cdot,\cdot)$, $b(\cdot,\cdot)$, the trilinear form $c(\cdot;\cdot,\cdot)$, and the norms $\|\cdot\|_{\mathbf{V}}$, $\|\cdot\|_Q$ by defining

$$a(\mathbf{u},\mathbf{v}) =: \sum_{E\in\Omega_h} a^E(\mathbf{u},\mathbf{v}) \qquad \text{for all } \mathbf{u},\mathbf{v}\in\mathbf{V},$$

$$b(\mathbf{v},q) =: \sum_{E\in\Omega_h} b^E(\mathbf{v},q) \qquad \text{for all } \mathbf{v}\in\mathbf{V} \text{ and } q\in Q,$$

$$c(\mathbf{w};\,\mathbf{u},\mathbf{v}) =: \sum_{E\in\Omega_h} c^E(\mathbf{w};\,\mathbf{u},\mathbf{v}) \qquad \text{for all } \mathbf{w},\mathbf{u},\mathbf{v}\in\mathbf{V},$$

and

$$\|\mathbf{v}\|_{\mathbf{V}} =: \left(\sum_{E\in\Omega_h} \|\mathbf{v}\|^2_{\mathbf{V},E}\right)^{1/2} \text{ for all } \mathbf{v}\in\mathbf{V}, \quad \|q\|_Q =: \left(\sum_{E\in\Omega_h} \|q\|^2_{Q,E}\right)^{1/2} \text{ for all } q\in Q.$$

Regarding $b(\cdot,\cdot)$, we simply set

$$b(\mathbf{v},q) = \sum_{E\in\Omega_h} b^E(\mathbf{v},q) = \sum_{E\in\Omega_h} \int_E \operatorname{div}\mathbf{v}\, q \,\mathrm{d}E \qquad \text{for all } \mathbf{v}\in\mathbf{V}_h,\ q\in Q_h; \tag{23}$$

i.e., as noticed in [15] we do not introduce any approximation of the bilinear form. We notice that (23) is computable from the DoFs $\mathbf{D_V 1}$, $\mathbf{D_V 2}$, and $\mathbf{D_V 4}$, since q is polynomial in each element $E\in\Omega_h$. We now define discrete versions of the forms $a(\cdot,\cdot)$ (cf. (4)) and $c(\cdot;\cdot,\cdot)$ (cf. (6)) that need to be dealt with in a more careful way. First we note that for an arbitrary pair $(\mathbf{u},\mathbf{v})\in\mathbf{V}_h^E\times\mathbf{V}_h^E$, the quantity $a^E(\mathbf{u},\mathbf{v})$ is not computable. Therefore, following a standard procedure in the VEM framework, we define a computable discrete local bilinear form

$$a_h^E(\cdot,\cdot)\colon \mathbf{V}_h^E\times\mathbf{V}_h^E\to\mathbb{R} \tag{24}$$

approximating the continuous form $a^E(\cdot,\cdot)$ and defined by

$$a_h^E(\mathbf{u},\mathbf{v}) := a^E\left(\Pi_{\mathrm{k}}^{\nabla,\mathrm{E}}\,\mathbf{u},\,\Pi_{\mathrm{k}}^{\nabla,\mathrm{E}}\,\mathbf{v}\right) + \mathcal{S}^E\left((I-\Pi_{\mathrm{k}}^{\nabla,\mathrm{E}})\mathbf{u},\,(I-\Pi_{\mathrm{k}}^{\nabla,\mathrm{E}})\mathbf{v}\right) \tag{25}$$

for all $\mathbf{u},\mathbf{v}\in\mathbf{V}_h^E$, where the (symmetric) stabilizing bilinear form $\mathcal{S}^E\colon \mathbf{V}_h^E\times\mathbf{V}_h^E\to\mathbb{R}$ satisfies (see Remark 3.3)

$$\alpha_* a^E(\mathbf{v},\mathbf{v}) \le \mathcal{S}^E(\mathbf{v},\mathbf{v}) \le \alpha^* a^E(\mathbf{v},\mathbf{v}) \qquad \text{for all } \mathbf{v}\in\mathbf{V}_h \text{ s.t. } \Pi_k^{\nabla,E}\mathbf{v}=\mathbf{0}, \tag{26}$$

with α_* and α^* positive constants independent of the element E. It is straightforward to check that definition (14) and properties (26) imply

- *k-consistency:* for all $\mathbf{q}_k\in[\mathbb{P}_k(E)]^2$ and $\mathbf{v}\in\mathbf{V}_h^K$,

$$a_h^E(\mathbf{q}_k,\mathbf{v}) = a^E(\mathbf{q}_k,\mathbf{v}); \tag{27}$$

- *stability:* there exist two positive constants α_* and α^*, independent of h and E, such that for all $\mathbf{v}\in\mathbf{V}_h^E$, it holds that

$$\alpha_* a^E(\mathbf{v},\mathbf{v}) \le a_h^E(\mathbf{v},\mathbf{v}) \le \alpha^* a^E(\mathbf{v},\mathbf{v}). \tag{28}$$

Remark 3.3. Condition (26) essentially requires the stabilizing term $\mathcal{S}^E(\mathbf{v}_h,\mathbf{v}_h)$ to scale as $a^E(\mathbf{v}_h,\mathbf{v}_h)$. For instance, following the most standard VEM choice (cf. [11, 12, 14]), denoting with $\vec{\mathbf{u}}_h$, $\vec{\mathbf{v}}_h\in\mathbb{R}^{N_{DoFs,E}}$ the vectors containing the values of the $N_{DoFs,E}$ DoFs associated to $\mathbf{u}_h,\mathbf{v}_h\in\mathbf{V}_h^E$, we set

$$\mathcal{S}^E(\mathbf{u}_h,\mathbf{v}_h) = \alpha^E\,\vec{\mathbf{u}}_h^T\vec{\mathbf{v}}_h,$$

where α^E is a suitable positive constant. For example, in the numerical tests presented in section 5, we have chosen α^E as the mean value of the nonzero eigenvalues of the matrix stemming from the term $a^E(\Pi_{\mathrm{k}}^{\nabla,\mathrm{E}}\,\mathbf{u}_h,\,\Pi_{\mathrm{k}}^{\nabla,\mathrm{E}}\,\mathbf{v}_h)$ in (25).

Finally we define the global approximated bilinear form $a_h(\cdot,\cdot)\colon \mathbf{V}_h\times\mathbf{V}_h\to\mathbb{R}$ by simply summing the local contributions:

$$a_h(\mathbf{u}_h,\mathbf{v}_h) := \sum_{E\in\Omega_h} a_h^E(\mathbf{u}_h,\mathbf{v}_h) \qquad \text{for all } \mathbf{u}_h,\mathbf{v}_h\in\mathbf{V}_h. \tag{29}$$

For the approximation of the local trialinear form $c^E(\cdot;\,\cdot,\cdot)$, we set

$$c_h^E(\mathbf{w}_h;\,\mathbf{u}_h,\mathbf{v}_h) := \int_E \left[\left(\boldsymbol{\Pi}_{\mathrm{k\text{-}1}}^{0,\mathrm{E}}\,\boldsymbol{\nabla}\mathbf{u}_h\right)\left(\Pi_{\mathrm{k}}^{0,\mathrm{E}}\,\mathbf{w}_h\right)\right]\cdot\Pi_{\mathrm{k}}^{0,\mathrm{E}}\,\mathbf{v}_h\,\mathrm{d}E \quad \text{for all } \mathbf{w}_h,\mathbf{u}_h,\mathbf{v}_h\in\mathbf{V}_h \tag{30}$$

and note that all quantities in (30) are computable, in the sense of Proposition 3.2. As usual we define the global approximated trilinear form by adding the local contributions:

$$c_h(\mathbf{w}_h;\,\mathbf{u}_h,\mathbf{v}_h) := \sum_{E\in\Omega_h} c_h^E(\mathbf{w}_h;\,\mathbf{u}_h,\mathbf{v}_h) \qquad \text{for all } \mathbf{w}_h,\mathbf{u}_h,\mathbf{v}_h\in\mathbf{V}_h. \tag{31}$$

We first notice that the form $c_h(\cdot;\,\cdot,\cdot)$ is immediately extendable to the whole $\mathbf{V}$ (simply apply the same definition for any $\mathbf{w},\mathbf{u},\mathbf{v}\in\mathbf{V}$). Moreover, we now show that it is continuous on $\mathbf{V}$, uniformly in h.

PROPOSITION 3.3. *Let*

$$\widehat{C}_h := \sup_{\mathbf{w},\mathbf{u},\mathbf{v}\in\mathbf{V}} \frac{|c_h(\mathbf{w};\,\mathbf{u},\mathbf{v})|}{\|\mathbf{w}\|_{\mathbf{V}}\|\mathbf{u}\|_{\mathbf{V}}\|\mathbf{v}\|_{\mathbf{V}}}. \tag{32}$$

Then $\widehat{C}_h$ is uniformly bounded, i.e., the trilinear form $c_h(\cdot;\,\cdot,\cdot)$ is uniformly continuous with respect to h.

Proof. By a direct computation it holds that

$$\begin{aligned} c_h(\mathbf{w};\,\mathbf{u},\mathbf{v}) &= \sum_{E\in\Omega_h} c_h^E(\mathbf{w};\,\mathbf{u},\mathbf{v}) = \sum_{E\in\Omega_h}\int_E \left[\left(\boldsymbol{\Pi}^{0,\mathrm{E}}_{\mathrm{k\text{-}1}}\,\boldsymbol{\nabla}\mathbf{u}\right)\left(\Pi^{0,\mathrm{E}}_{\mathrm{k}}\,\mathbf{w}\right)\right]\cdot\Pi^{0,\mathrm{E}}_{\mathrm{k}}\,\mathbf{v}\,\mathrm{d}E \\ &\le \sum_{i,j=1}^{2}\sum_{E\in\Omega_h}\left\|\Pi^{0,\mathrm{E}}_{\mathrm{k}}\,\frac{\partial\mathbf{u}_i}{\partial x_j}\right\|_{0,E}\left\|\Pi^{0,\mathrm{E}}_{\mathrm{k}}\,\mathbf{w}_j\right\|_{L^4(E)}\left\|\Pi^{0,\mathrm{E}}_{\mathrm{k}}\,\mathbf{v}_i\right\|_{L^4(E)}, \end{aligned} \tag{33}$$

where the last inequality follows by using the Hölder inequality. Let us analyze each term in the right-hand side of (33). Employing the continuity of the projection $\Pi^{0,\mathrm{E}}_{\mathrm{k}}$ with respect to the L^2-norm, we easily get

$$\left\|\Pi^{0,\mathrm{E}}_{\mathrm{k}}\,\frac{\partial\mathbf{u}_i}{\partial x_j}\right\|_{0,E} \le \left\|\frac{\partial\mathbf{u}_i}{\partial x_j}\right\|_{0,E}. \tag{34}$$

For the second term (and analogously for the third one) we get

$$\begin{aligned} \left\|\Pi^{0,\mathrm{E}}_{\mathrm{k}}\,\mathbf{w}_j\right\|_{L^4(E)} &\le Ch_E^{-\frac{1}{2}}\left\|\Pi^{0,\mathrm{E}}_{\mathrm{k}}\,\mathbf{w}_j\right\|_{0,E} && \text{(inverse estimate for polynomials)} \\ &\le Ch_E^{-\frac{1}{2}}\left\|\mathbf{w}_j\right\|_{0,E} && \text{(continuity of } \Pi^{0,\mathrm{E}}_{\mathrm{k}} \text{ with respect to } \|\cdot\|_{0,E}) \\ &\le Ch_E^{-\frac{1}{2}}\left\|1\right\|_{L^4(E)}\left\|\mathbf{w}_j\right\|_{L^4(E)} && \text{(Hölder inequality)} \\ &\le Ch_E^{-\frac{1}{2}}\,(h_E^2)^{\frac{1}{4}}\left\|\mathbf{w}_j\right\|_{L^4(E)} && \text{(definition of } h_E) \\ &\le C\left\|\mathbf{w}_j\right\|_{L^4(E)}. \end{aligned} \tag{35}$$

Combining (34) and (35) in (33) we obtain

$$c_h(\mathbf{w};\,\mathbf{u},\mathbf{v}) \le C\sum_{i,j=1}^{2}\sum_{E\in\Omega_h}\left\|\frac{\partial\mathbf{u}_i}{\partial x_j}\right\|_{0,E}\left\|\mathbf{w}_j\right\|_{L^4(E)}\left\|\mathbf{v}_i\right\|_{L^4(E)}. \tag{36}$$

Now applying the Hölder inequality (for sequences) we get

$$\begin{aligned} c_h(\mathbf{w};\,\mathbf{u},\mathbf{v}) &\le C\sum_{i,j=1}^{2}\left(\sum_{E\in\Omega_h}\left\|\frac{\partial\mathbf{u}_i}{\partial x_j}\right\|_{0,E}^2\right)^{\frac{1}{2}}\left(\sum_{E\in\Omega_h}\|\mathbf{w}_j\|_{L^4(E)}^4\right)^{\frac{1}{4}}\left(\sum_{E\in\Omega_h}\|\mathbf{v}_i\|_{L^4(E)}^4\right)^{\frac{1}{4}} \\ &\le C\sum_{i,j=1}^{2}\left\|\frac{\partial\mathbf{u}_i}{\partial x_j}\right\|_{0}\left\|\mathbf{w}_j\right\|_{L^4(\Omega)}\left\|\mathbf{v}_i\right\|_{L^4(\Omega)}. \end{aligned} \tag{37}$$

Finally, since $H^1(\Omega)\subset L^4(\Omega)$, by Sobolev embedding it holds that

$$c_h(\mathbf{w};\,\mathbf{u},\mathbf{v}) \le \widehat{C}_h\,\|\mathbf{u}\|_{\mathbf{V}}\|\mathbf{w}\|_{\mathbf{V}}\|\mathbf{v}\|_{\mathbf{V}},$$

where the constant $\widehat{C}_h$ does not depend on h. ∎

We can also define the local discrete skew-symmetric trilinear form $\widetilde{c}_h^E(\cdot;\,\cdot,\cdot)\colon \mathbf{V}\times\mathbf{V}\times\mathbf{V}\to\mathbb{R}$ by simply setting

$$\widetilde{c}_h^E(\mathbf{w};\,\mathbf{u},\mathbf{v}) := \frac{1}{2}c_h^E(\mathbf{w};\,\mathbf{u},\mathbf{v}) - \frac{1}{2}c_h^E(\mathbf{w};\,\mathbf{v},\mathbf{u}) \qquad \text{for all } \mathbf{w},\mathbf{u},\mathbf{v}\in\mathbf{V} \tag{38}$$

with obvious global extension

$$\widetilde{c}_h(\mathbf{w};\,\mathbf{u},\mathbf{v}) := \sum_{E\in\Omega_h}\widetilde{c}_h^E(\mathbf{w};\,\mathbf{u},\mathbf{v}) \qquad \text{for all } \mathbf{w},\mathbf{u},\mathbf{v}\in\mathbf{V}, \tag{39}$$

which is (obviously) still continuous and computable.

The last step consists in constructing a computable approximation of the right-hand side $(\mathbf{f},\,\mathbf{v})$ in (7). We define the approximated load term $\mathbf{f}_h$ as

$$\mathbf{f}_h := \Pi_k^{0,E}\mathbf{f} \qquad \text{for all } E\in\Omega_h, \tag{40}$$

and consider

$$(\mathbf{f}_h,\mathbf{v}_h) = \sum_{E\in\Omega_h}\int_E \mathbf{f}_h\cdot\mathbf{v}_h\,\mathrm{d}E = \sum_{E\in\Omega_h}\int_E \Pi_k^{0,E}\mathbf{f}\cdot\mathbf{v}_h\,\mathrm{d}E = \sum_{E\in\Omega_h}\int_E \mathbf{f}\cdot\Pi_k^{0,E}\mathbf{v}_h\,\mathrm{d}E. \tag{41}$$

We observe that (41) can be computed from $\mathbf{D}_\mathbf{V}$ for all $\mathbf{v}_h\in\mathbf{V}_h$ (see Proposition 3.2), once a suitable quadrature rule is available for polygonal domains. Details on such an issue can be found, for instance, in [49, 44, 31].

Remark 3.4. We highlight that the construction introduced in this paper is not peculiar to the two-dimensional case and could be used to develop a three-dimensional virtual element scheme (see the appendix in [15] for details on the extension to three dimensions). The theoretical analysis of the three-dimensional case (in the diffusion dominated regime) could follow along the same lines as for the two-dimensional case, although some technical steps (such as, for instance, interpolation estimates in three dimensions) could need a modified proof.

3.3. The discrete problem. We are now ready to state the proposed discrete problem. Referring to (20), (21), (29), (39), and (23), we consider the *virtual element problem*:

$$\begin{cases} \text{find } (\mathbf{u}_h,p_h)\in\mathbf{V}_h\times Q_h, \text{ s.t.} & \\ \nu\, a_h(\mathbf{u}_h,\mathbf{v}_h) + \widetilde{c}_h(\mathbf{u}_h;\,\mathbf{u}_h,\mathbf{v}_h) + b(\mathbf{v}_h,p_h) = (\mathbf{f}_h,\mathbf{v}_h) & \text{for all } \mathbf{v}_h\in\mathbf{V}_h, \\ b(\mathbf{u}_h,q_h) = 0 & \text{for all } q_h\in Q_h. \end{cases} \tag{42}$$

We point out that the symmetry of $a_h(\cdot,\cdot)$ together with (28) easily implies that $a_h(\cdot,\cdot)$ is continuous and coercive with respect to the $\mathbf{V}$-norm. Moreover, as a direct consequence of Proposition 4.3 in [15], we have the following stability result.

PROPOSITION 3.4. *Given the discrete spaces $\mathbf{V}_h$ and Q_h defined in* (20) *and* (21)*, there exists a positive $\widehat{\beta}$, independent of h, such that*

$$\sup_{\mathbf{v}_h\in\mathbf{V}_h\,\mathbf{v}_h\neq\mathbf{0}} \frac{b(\mathbf{v}_h,q_h)}{\|\mathbf{v}_h\|_\mathbf{V}} \geq \widehat{\beta}\|q_h\|_Q \qquad \textit{for all } q_h\in Q_h. \tag{43}$$

In particular, the inf-sup condition of Proposition 3.4, along with property (22), implies that

$$\operatorname{div}\mathbf{V}_h = Q_h.$$

The well-posedness of virtual problem (42) is a consequence of the coercivity property of $a_h(\cdot,\cdot)$, the skew-symmetry of $\widetilde{c}_h(\cdot;\cdot,\cdot)$, and the inf-sup condition (43). We have the following theorem.

THEOREM 3.5. *Assuming that*

$$\gamma_h := \frac{\widehat{C}_h \, \|\mathbf{f}_h\|_{-1}}{\alpha_*^2 \, \nu^2} \leq r < 1, \tag{44}$$

problem (42) *has a unique solution* $(\mathbf{u}_h, p_h) \in \mathbf{V}_h \times Q_h$ *such that*

$$\|\mathbf{u}_h\|_{\mathbf{V}} \leq \frac{\|\mathbf{f}_h\|_{H^{-1}}}{\alpha_* \, \nu}. \tag{45}$$

Moreover, as observed in [15], introducing the discrete kernel

$$\mathbf{Z}_h := \{\mathbf{v}_h \in \mathbf{V}_h \quad \text{s.t.} \quad b(\mathbf{v}_h, q_h) = 0 \quad \text{for all } q_h \in Q_h\},$$

recalling (22) it follows that

$$\mathbf{Z}_h \subseteq \mathbf{Z}. \tag{46}$$

Problem (42) can be also formulated in the equivalent kernel form

$$\begin{cases} \text{find } \mathbf{u}_h \in \mathbf{Z}_h, \text{ s.t.} \\ \nu \, a_h(\mathbf{u}_h, \mathbf{v}_h) + \widetilde{c}_h(\mathbf{u}_h;\, \mathbf{u}_h, \mathbf{v}_h) = (\mathbf{f}_h, \mathbf{v}_h) \qquad \text{for all } \mathbf{v}_h \in \mathbf{Z}_h. \end{cases} \tag{47}$$

Remark 3.5. An alternative choice for the discretization (42) is to replace the skew-symmetric form $\widetilde{c}_h(\cdot;\cdot,\cdot)$ with $c_h(\cdot;\cdot,\cdot)$. With that choice, a theoretical analysis can be developed using the guidelines in [41] in connection with the same tools and ideas of section 4. Here we prefer to consider the choice (42), which allows for a more direct stability argument. Nevertheless, in the numerical tests of section 5 we will investigate both possibilities.

Remark 3.6. An additional interesting consequence of property (46) is that, following [15, 52], the proposed virtual elements can accommodate both the Stokes (or Navier–Stokes) and the Darcy problems simultaneously. Indeed, due to property (46), the proposed velocity-pressure coupling turns out to be stable not only for the Stokes problem, but also for the Darcy problem. This yields an interesting advantage in complex flow problems where both equations are present: the same spaces can be used in the whole computational domain. As a consequence, the implementation of the method and the enforcement of the interface conditions are greatly simplified (see also section 5.6).

4. Theoretical analysis.

4.1. Interpolation estimates. In this section we prove that the following interpolation estimate holds for the enhanced space $\mathbf{V}_h$. Since the proof is quite involved, we divide it into three steps. Interpolation proofs for more standard H^1-conforming virtual element spaces can be found (with different degrees of generalization) in [43, 27, 14, 21].

THEOREM 4.1. *Let* $\mathbf{v} \in H^{s+1}(\Omega) \cap \mathbf{V}$ *for* $0 < s \leq k$. *Then there exists* $\mathbf{v}_I \in \mathbf{V}_h$ *such that*

$$\|\mathbf{v} - \mathbf{v}_I\|_0 + h \, \|\mathbf{v} - \mathbf{v}_I\|_{\mathbf{V}} \leq C \, h^{s+1} \, |\mathbf{v}|_{s+1},$$

where the constant C *depends only on the degree* k *and the shape regularity constants* ϱ, c *(see assumptions* (A1) *and* (A2) *of section* 3.1*).*

Proof. Step 1. Let $\mathbf{w}_I$ be the approximant function of $\mathbf{v}$ in the space $\mathbf{W}_h$ obtained by gluing the local spaces $\mathbf{W}_h^E$ (cf. (16) and Proposition 4.2 in [15]); then it holds that

$$\|\mathbf{v}-\mathbf{w}_I\|_0 + h\,\|\mathbf{v}-\mathbf{w}_I\|_{\mathbf{V}} \le C\,h^{s+1}\,|\mathbf{v}|_{s+1}. \tag{48}$$

Now let $\mathbf{v}_I \in \mathbf{V}_h$ be the interpolant of $\mathbf{w}_I$ in the sense of the DoFs $\mathbf{D_V}$, so that

$$\mathbf{D_V}(\mathbf{v}_I) = \mathbf{D_V}(\mathbf{w}_I). \tag{49}$$

Let us define $\boldsymbol{\vartheta} := \mathbf{v}_I - \mathbf{w}_I$; then for every element $E \in \Omega_h$ the following facts hold:

- Since $\mathbf{v}_I$ and $\mathbf{w}_I$ are polynomials of degree k on ∂E, by definition of $\mathbf{D_V 1}$ and $\mathbf{D_V 2}$, we have
$$\boldsymbol{\vartheta} = \mathbf{0} \qquad \text{on } \partial E. \tag{50}$$
- Since $\operatorname{div}\mathbf{v}_I$ and $\operatorname{div}\mathbf{w}_I$ are polynomials of degree $k-1$ in E, by definition of $\mathbf{D_V 4}$ and homogeneous boundary data (50), we get
$$\operatorname{div}\boldsymbol{\vartheta} = 0 \qquad \text{in } E. \tag{51}$$
- Let $d^E(\cdot,\cdot)\colon H_0^1(E)\times\mathcal{G}_k^{\oplus}(E)\to\mathbb{R}$ be given by
$$d^E(\mathbf{v},\mathbf{g}_{\mathrm{k}}^{\oplus}) = \int_E \mathbf{v}\cdot\mathbf{g}_{\mathrm{k}}^{\oplus}\,\mathrm{d}E \qquad \text{for all } \mathbf{v}\in H_0^1(E) \text{ and } \mathbf{g}_{\mathrm{k}}^{\oplus}\in\mathcal{G}_{\mathrm{k}}^{\oplus}(\mathrm{E}).$$
Then by definition of $\mathbf{D_V 3}$, we infer
$$d^E(\boldsymbol{\vartheta},\mathbf{g}_{\mathrm{k\text{-}2}}^{\oplus}) = 0 \qquad \text{for all } \mathbf{g}_{\mathrm{k\text{-}2}}^{\oplus}\in\mathcal{G}_{\mathrm{k\text{-}2}}^{\oplus}(\mathrm{E}). \tag{52}$$
Now we recall that, for any $\mathbf{v}_h\in\mathbf{V}_h$, the quantity $\Pi_{\mathrm{k}}^{\nabla,\mathrm{E}}\mathbf{v}_h$ depends only on the values of $\mathbf{D_V}(\mathbf{v}_h)$; see Proposition 3.2. Therefore, using (49), we have that $\Pi_{\mathrm{k}}^{\nabla,\mathrm{E}}\mathbf{v}_I = \Pi_{\mathrm{k}}^{\nabla,\mathrm{E}}\mathbf{w}_I$. As a consequence, by definition of $\mathbf{V}_h^E$ it holds that
$$d^E(\boldsymbol{\vartheta},\mathbf{g}^{\perp}) = \int_E\left(\Pi_{\mathrm{k}}^{\nabla,\mathrm{E}}\mathbf{v}_I-\mathbf{w}_I\right)\cdot\mathbf{g}^{\perp}\,\mathrm{d}E = \int_E\left(\Pi_{\mathrm{k}}^{\nabla,\mathrm{E}}\mathbf{w}_I-\mathbf{w}_I\right)\cdot\mathbf{g}^{\perp}\,\mathrm{d}E \tag{53}$$
for all $\mathbf{g}^{\perp}\in\mathcal{G}_{\mathrm{k}}^{\oplus}(\mathrm{E})\setminus\mathcal{G}_{\mathrm{k\text{-}2}}^{\oplus}(\mathrm{E})$. Thus, by (52) and (53),
$$d^E(\boldsymbol{\vartheta},\mathbf{g}_{\mathrm{k}}^{\oplus}) = (\boldsymbol{\chi},\mathbf{g}_{\mathrm{k}}^{\oplus}) \qquad \text{for all } \mathbf{g}_{\mathrm{k}}^{\oplus}\in\mathcal{G}_{\mathrm{k}}^{\oplus}(\mathrm{E}), \tag{54}$$
where
$$\boldsymbol{\chi} \text{ is the } L^2\text{-projection of } \left(\Pi_{\mathrm{k}}^{\nabla,\mathrm{E}}\mathbf{w}_I-\mathbf{w}_I\right) \text{ onto } \mathcal{G}_{\mathrm{k}}^{\oplus}(\mathrm{E})\setminus\mathcal{G}_{\mathrm{k\text{-}2}}^{\oplus}(\mathrm{E}). \tag{55}$$
- By definition of $\mathbf{W}_h^E$ and $\mathbf{V}_h^E$ there exist $\widehat{s}\in L_0^2(E)$ and $\widehat{\mathbf{g}}\in\mathcal{G}_{\mathrm{k}}^{\oplus}(\mathrm{E})$ such that
$$a^E(\boldsymbol{\vartheta},\mathbf{v}) + b^E(\mathbf{v},\widehat{s}) + d^E(\mathbf{v},\widehat{\mathbf{g}}) = 0 \qquad \text{for all } \mathbf{v}\in H_0^1(E). \tag{56}$$

Combining (50), (51), (54), and (56), it follows that $(\boldsymbol{\vartheta},\widehat{s},\widehat{\mathbf{g}})$ solves the problem

$$\begin{cases} \text{find } (\boldsymbol{\vartheta},\widehat{s},\widehat{\mathbf{g}})\in[H_0^1(E)]^2\times L_0^2(E)\times\mathcal{G}_{\mathrm{k}}^{\oplus}(\mathrm{E}), \text{ s.t.} & \\ a^E(\boldsymbol{\vartheta},\boldsymbol{\psi}) + b^E(\boldsymbol{\psi},\widehat{s}) + d^E(\boldsymbol{\psi},\widehat{\mathbf{g}}) = 0 & \text{for all } \boldsymbol{\psi}\in[H_0^1(E)]^2, \\ b^E(\boldsymbol{\vartheta},q) = 0 & \text{for all } q\in L_0^2(E), \\ d^E(\boldsymbol{\vartheta},\mathbf{h}) = (\boldsymbol{\chi},\mathbf{h}) & \text{for all } \mathbf{h}\in\mathcal{G}_{\mathrm{k}}^{\oplus}(\mathrm{E}). \end{cases} \tag{57}$$

Step 2. We now analyze the well-posedness of problem (57). We consider $[H^1_0(E)]^2$ and $L^2(E)$ endowed with the H^1- and the L^2-norm, respectively, and $\mathcal{G}^{\oplus}_{\mathrm{k}}(\mathrm{E})$ endowed with the scaled norm

$$\|\mathbf{h}\|_{\mathcal{G}^{\oplus}_{\mathrm{k}}(\mathrm{E})} := h_E \, \|\mathbf{h}\|_{0,E} \qquad \text{for all } \mathbf{h} \in \mathcal{G}^{\oplus}_{\mathrm{k}}(\mathrm{E}).$$

Then for all $\boldsymbol{\psi} \in [H^1_0(E)]^2$ and $\mathbf{h} \in \mathcal{G}^{\oplus}_{\mathrm{k}}(\mathrm{E})$,

$$d^E(\boldsymbol{\psi}, \mathbf{h}) = \int_E \boldsymbol{\psi} \cdot \mathbf{h} \, \mathrm{d}E \le \|\boldsymbol{\psi}\|_{0,E} \|\mathbf{h}\|_{0,E} \le c_{\mathrm{cont}} \, |\boldsymbol{\psi}|_{1,E} \, h^E \|\mathbf{h}\|_{0,E}, \tag{58}$$

where the last inequality follows by a scaled Poincaré inequality. Therefore all the involved bilinear forms are continuous. By the theory of problems in mixed form [20], due to the coercivity of $a^E(\cdot,\cdot)$ the well-posedness of problem (57) will follow if we show an inf-sup condition for the form

$$b^E(\cdot,\cdot) + d^E(\cdot,\cdot) \, : \; [H^1_0(E)]^2 \times \big(L^2_0(E) \times \mathcal{G}^{\oplus}_{\mathrm{k}}(\mathrm{E})\big) \to \mathbb{R}.$$

In other words, for all $(q, \mathbf{h}) \in L^2_0(E) \times \mathcal{G}^{\oplus}_{\mathrm{k}}(\mathrm{E})$ we have to find $\boldsymbol{\varphi} \in H^1_0(E)$ such that

$$\begin{cases} |\boldsymbol{\varphi}|_{1,E} \le b_0 \, (\|q\|_{0,E} + \|\mathbf{h}\|_{\mathcal{G}^{\oplus}_{\mathrm{k}}(\mathrm{E})}), \\ b^E(\boldsymbol{\varphi}, q) + d^E(\boldsymbol{\varphi}, \mathbf{h}) \ge c_0 \, (\|q\|_{0,E} + \|\mathbf{h}\|_{\mathcal{G}^{\oplus}_{\mathrm{k}}(\mathrm{E})})^2 \end{cases} \tag{59}$$

for suitable uniform positive constants b_0, c_0. It is well known (see [20]) that for all $q \in L^2_0(E)$ there exists $\boldsymbol{\varphi}_1 \in [H^1_0(E)]^2$ such that

$$\begin{cases} |\boldsymbol{\varphi}_1|_{1,E} \le b_1 \, \|q\|_{0,E}, \\ b^E(\boldsymbol{\varphi}_1, q) \ge c_1 \, \|q\|^2_{0,E}. \end{cases} \tag{60}$$

Now let $T_E \subset E$ be an equilateral triangle inscribed in the ball B_E (cf. assumption (A1)). Then for all polynomial $p \in \mathbb{P}_k(E)$, it holds that $\|p\|_{0,E} \le C \|p\|_{0,T_E}$ for a suitable uniform constant C. Let $\mathbf{h} \in \mathcal{G}^{\oplus}_{\mathrm{k}}(\mathrm{E})$, and define

$$q := \mathrm{rot}(\mathbf{h}) \qquad \text{and} \qquad \boldsymbol{\varphi}_2 := h^4_E \, \mathbf{curl}(bq),$$

where $b \in \mathbb{P}_3(T_E)$ denotes the standard cubic bubble in T_E with unitary maximum value (extended to zero in $E \setminus T_E$). Therefore, we get

$$\begin{aligned} d^E(\boldsymbol{\varphi}_2, \mathbf{h}) &= h^4_E \int_E \mathbf{curl}(bq) \cdot \mathbf{h} \, \mathrm{d}E = h^4_E \int_{T_E} \mathbf{curl}(bq) \cdot \mathbf{h} \, \mathrm{d}E = h^4_E \int_{T_E} bq \, \mathrm{rot}(\mathbf{h}) \, \mathrm{d}E \\ &= h^4_E \int_{T_E} b \, \mathrm{rot}(\mathbf{h})^2 \, \mathrm{d}E \ge C h^4_E \, \|\mathrm{rot}(\mathbf{h})\|^2_{0,T_E}. \end{aligned} \tag{61}$$

Since $\mathrm{rot}\colon \mathcal{G}^{\oplus}_k(T_E) \to \mathbb{P}_{k-1}(T_E)$ is an isomorphism (see [9]), a scaling argument for polynomials on the triangle T_E yields $\|\mathrm{rot}(\mathbf{h})\|_{0,T_E} \ge h_E^{-1} \|\mathbf{h}\|_{0,T_E}$. Thus using (61) we find

$$d^E(\boldsymbol{\varphi}_2, \mathbf{h}) \ge C \, h^4_E \, h_E^{-2} \, \|\mathbf{h}\|^2_{0,T_E} \ge C \, h^2_E \, \|\mathbf{h}\|^2_{0,E} = C \, \|\mathbf{h}\|^2_{\mathcal{G}^{\oplus}_{\mathrm{k}}(\mathrm{E})}. \tag{62}$$

Moreover, using an inverse estimate for the polynomials bq and $\mathbf{h}$ (cf. [22], for instance),

$$
\begin{aligned}
|\boldsymbol{\varphi}_2|_{1,E} &= h_E^4\,|\mathbf{curl}(bq)|_{1,E} \le C h_E^4\; h_E^{-2}\|bq\|_{0,E} \le C\,h_E^2\|q\|_{0,E} \\
&= C\,h_E^2\|\mathrm{rot}(\mathbf{h})\|_{0,E} \le C\,h_E\,\|\mathbf{h}\|_{0,E} = C\|\mathbf{h}\|_{\mathcal{G}_{\mathrm{k}}^{\oplus}(\mathrm{E})}.
\end{aligned} \tag{63}
$$

Therefore by (62) and (63) for all $\mathbf{h} \in \mathcal{G}_{\mathrm{k}}^{\oplus}(\mathrm{E})$ we find $\boldsymbol{\varphi}_2 \in H_0^1(E)$ such that

$$
\begin{cases}
|\boldsymbol{\varphi}_2|_{1,E} \le b_2\,\|\mathbf{h}\|_{\mathcal{G}_{\mathrm{k}}^{\oplus}(\mathrm{E})}, \\
d^E(\boldsymbol{\varphi}_2, \mathbf{h}) \ge c_2\,\|\mathbf{h}\|^2_{\mathcal{G}_{\mathrm{k}}^{\oplus}(\mathrm{E})}.
\end{cases} \tag{64}
$$

Recalling (59), let us set $\boldsymbol{\varphi} := \boldsymbol{\varphi}_1 + \xi\,\boldsymbol{\varphi}_2$ (cf. (60) and (64)), where ξ is a positive constant. Then, it is clear that

$$
|\boldsymbol{\varphi}|_{1,E} \le |\boldsymbol{\varphi}_1|_{1,E} + |\boldsymbol{\varphi}_2|_{1,E} \le \max\{b_1,\, b_2\}\,(1+\xi)(\|q\|_{0,E} + \|\mathbf{h}\|_{\mathcal{G}_{\mathrm{k}}^{\oplus}(\mathrm{E})}). \tag{65}
$$

Moreover, by (58) and since $\operatorname{div}\mathbf{curl} = 0$, we have

$$
\begin{aligned}
b^E(\boldsymbol{\varphi}, q) + d^E(\boldsymbol{\varphi}, \mathbf{h}) &= b^E(\boldsymbol{\varphi}_1, q) + d^E(\boldsymbol{\varphi}_1, \mathbf{h}) + \xi\,b^E(\boldsymbol{\varphi}_2, q) + \xi\,d^E(\boldsymbol{\varphi}_2, \mathbf{h}) \\
&= b^E(\boldsymbol{\varphi}_1, q) + d^E(\boldsymbol{\varphi}_1, \mathbf{h}) + \xi\,d^E(\boldsymbol{\varphi}_2, \mathbf{h}) \\
&\ge c_1\,\|q\|^2_{0,E} + c_2\,\xi\,\|\mathbf{h}\|^2_{\mathcal{G}_{\mathrm{k}}^{\oplus}(\mathrm{E})} + d^E(\boldsymbol{\varphi}_1, \mathbf{h}) \\
&\ge c_1\,\|q\|^2_{0,E} + c_2\,\xi\,\|\mathbf{h}\|^2_{\mathcal{G}_{\mathrm{k}}^{\oplus}(\mathrm{E})} - c_{\mathrm{cont}}\,|\boldsymbol{\varphi}_1|_{1,E}\|\mathbf{h}\|_{\mathcal{G}_{\mathrm{k}}^{\oplus}(\mathrm{E})} \\
&\ge c_1\,\|q\|^2_{0,E} + c_2\,\xi\,\|\mathbf{h}\|^2_{\mathcal{G}_{\mathrm{k}}^{\oplus}(\mathrm{E})} - c_{\mathrm{cont}} b_1\,\|q\|_{0,E}\|\mathbf{h}\|_{\mathcal{G}_{\mathrm{k}}^{\oplus}(\mathrm{E})} \\
&\ge \left(c_1 - \frac{\varepsilon}{2} c_{\mathrm{cont}} b_1\right)\,\|q\|^2_{0,E} + \left(\xi\,c_2 - \frac{1}{2\varepsilon} c_{\mathrm{cont}} b_1\right)\,\|\mathbf{h}\|^2_{\mathcal{G}_{\mathrm{k}}^{\oplus}(\mathrm{E})}
\end{aligned} \tag{66}
$$

for any positive real number ε. Finally, setting

$$
\varepsilon := \frac{c_1}{c_{\mathrm{cont}} b_1} \qquad \text{and} \qquad \xi := \frac{c_{\mathrm{cont}}^2\, b_1^2}{c_1 c_2},
$$

by (65) and (66) we get (59).

Step 3. Since problem (57) is well-posed, the following stability estimate holds:

$$
|\boldsymbol{\vartheta}|_{1,E} + \|\widehat{s}\|_{0,E} + \|\widehat{\mathbf{g}}\|_{\mathcal{G}_{\mathrm{k}}^{\oplus}(\mathrm{E})} \le \|\boldsymbol{\chi}\|_{(\mathcal{G}_{\mathrm{k}}^{\oplus}(\mathrm{E}))^*},
$$

where

$$
\|\boldsymbol{\chi}\|_{(\mathcal{G}_{\mathrm{k}}^{\oplus}(\mathrm{E}))^*} := \sup_{\mathbf{h}\in\mathcal{G}_{\mathrm{k}}^{\oplus}(\mathrm{E}),\mathbf{h}\neq\mathbf{0}} \frac{(\boldsymbol{\chi}, \mathbf{h})}{\|\mathbf{h}\|_{\mathcal{G}_{\mathrm{k}}^{\oplus}(\mathrm{E})}} \le h_E^{-1}\,\|\boldsymbol{\chi}\|_{0,E}.
$$

Then, by the definition of $\boldsymbol{\chi}$ (see (55)) and by the continuity of the L^2-projection, we get

$$
|\boldsymbol{\vartheta}|_{1,E} \le h_E^{-1}\,\|\boldsymbol{\chi}\|_{0,E} \le h_E^{-1}\,\left\|\Pi_{\mathrm{k}}^{\nabla,\mathrm{E}}\,\mathbf{w}_I - \mathbf{w}_I\right\|_{0,E} \le C\left|\Pi_{\mathrm{k}}^{\nabla,\mathrm{E}}\,\mathbf{w}_I - \mathbf{w}_I\right|_{1,E},
$$

where the last inequality is justified since, by (14), the function $\Pi_{\mathrm{k}}^{\nabla,\mathrm{E}}\,\mathbf{w}_I - \mathbf{w}_I$ has zero mean value. Noting that $\Pi_{\mathrm{k}}^{\nabla,\mathrm{E}}$ is a projection with respect to the H^1-seminorm

and using a triangular inequality, from (48) we finally get

$$
\begin{aligned}
|\boldsymbol{\vartheta}|_{1,E} &\leq \left(\left| \Pi_{\mathrm{k}}^{\nabla,\mathrm{E}} (\mathbf{w}_I - \mathbf{v}) |_{1,E} \right| + \left| \mathbf{w}_I - \Pi_{\mathrm{k}}^{\nabla,\mathrm{E}} \mathbf{v} \right|_{1,E} \right) \\
&\leq \left(2\, |(\mathbf{w}_I - \mathbf{v})|_{1,E}| + \left| \mathbf{v} - \Pi_{\mathrm{k}}^{\nabla,\mathrm{E}} \mathbf{v} \right|_{1,E} \right) \\
&\leq C\, h_E^s\, |\mathbf{v}|_{s+1,E}.
\end{aligned} \tag{67}
$$

The proof now follows from (67) and again (48) by adding all the local contributions. For the L^2 estimate, for each polygon $E \in \Omega_h$, we have that $\boldsymbol{\vartheta} = \mathbf{0}$ on ∂E (see (50)). Hence, from (67) it holds that

$$
\|\boldsymbol{\vartheta}\|_{0,E} \leq C\, h_E\, |\boldsymbol{\vartheta}|_{1,E} \leq C\, h_E^{s+1}\, |\mathbf{v}|_{s+1,E},
$$

from which we easily infer the L^2 estimate. ∎

4.2. Convergence analysis. First let us recall a classical approximation result for $\mathbb{P}_k$ polynomials on star-shaped domains; see, for instance, [22].

LEMMA 4.2. *Let $E \in \Omega_h$, and let two real numbers s, p with $0 \leq s \leq k$ and $1 \leq p \leq \infty$. Then for all $\mathbf{u} \in [H^{s+1}(E)]^2$, there exists a polynomial function $\mathbf{u}_\pi \in [\mathbb{P}_k(E)]^2$, such that*

$$
\|\mathbf{u} - \mathbf{u}_\pi\|_{L^p(E)} + h_E |\mathbf{u} - \mathbf{u}_\pi|_{W^{1,p}(E)} \leq C h_E^{s+1} |\mathbf{u}|_{W^{s+1,p}(E)}, \tag{68}
$$

with C depending only on k and the shape regularity constant ϱ in assumption (A1).

Now we prove two technical lemmas.

LEMMA 4.3. *Let $\mathbf{v} \in H^{s+1}(\Omega) \cap \mathbf{V}$ with $0 \leq s \leq k$. Then for all $\mathbf{w} \in \mathbf{V}$ it holds that*

$$
|\widetilde{c}(\mathbf{v};\, \mathbf{v}, \mathbf{w}) - \widetilde{c}_h(\mathbf{v};\, \mathbf{v}, \mathbf{w})| \leq C\, h^s\, \left(\|\mathbf{v}\|_s + \|\mathbf{v}\|_{\mathbf{V}} + \|\mathbf{v}\|_{s+1} \right) \|\mathbf{v}\|_{s+1}\, \|\mathbf{w}\|_{\mathbf{V}}.
$$

Proof. First we set

$$
\begin{aligned}
\mu_1(\mathbf{w}) &:= \sum_{E \in \Omega_h} \left(c^E(\mathbf{v};\, \mathbf{v}, \mathbf{w}) - c_h^E(\mathbf{v};\, \mathbf{v}, \mathbf{w}) \right), \\
\mu_2(\mathbf{w}) &:= \sum_{E \in \Omega_h} \left(c^E(\mathbf{v};\, \mathbf{w}, \mathbf{v}) - c_h^E(\mathbf{v};\, \mathbf{w}, \mathbf{v}) \right);
\end{aligned} \tag{69}
$$

then by definition (38) and (39) it holds that

$$
\widetilde{c}(\mathbf{v};\, \mathbf{v}, \mathbf{w}) - \widetilde{c}_h(\mathbf{v};\, \mathbf{v}, \mathbf{w}) = \frac{1}{2} \big(\mu_1(\mathbf{w}) + \mu_2(\mathbf{w}) \big). \tag{70}
$$

We now analyze the two terms. For the term $\mu_1(\mathbf{w})$, by simple computations, we have

$$
\begin{aligned}
\mu_1(\mathbf{w}) &= \sum_{E \in \Omega_h} \int_E \left((\boldsymbol{\nabla} \mathbf{v})\, \mathbf{v} \cdot \mathbf{w} - \left(\boldsymbol{\Pi}_{\mathrm{k\text{-}1}}^{0,\mathrm{E}}\, \boldsymbol{\nabla} \mathbf{v} \right) \left(\Pi_{\mathrm{k}}^{0,\mathrm{E}}\, \mathbf{v} \right) \cdot \Pi_{\mathrm{k}}^{0,\mathrm{E}}\, \mathbf{w} \right) \mathrm{d}E \\
&= \sum_{E \in \Omega_h} \sum_{i,j=1}^{2} \int_E \left(\frac{\partial \mathbf{v}_i}{\partial x_j}\, \mathbf{v}_j\, \mathbf{w}_i - \left(\Pi_{k-1}^{0,E}\, \frac{\partial \mathbf{v}_i}{\partial x_j} \right) \left(\Pi_{\mathrm{k}}^{0,\mathrm{E}}\, \mathbf{v}_j \right) \Pi_{\mathrm{k}}^{0,\mathrm{E}}\, \mathbf{w}_i \right) \mathrm{d}E,
\end{aligned}
$$

from which it follows that

(71)
$$\mu_1(\mathbf{w}) = \sum_{E\in\Omega_h}\sum_{i,j=1}^{2}\int_E \left(\frac{\partial \mathbf{v}_i}{\partial x_j}\,\mathbf{v}_j\left[\left(I-\Pi_{\mathrm{k}}^{0,\mathrm{E}}\right)\mathbf{w}_i\right]\right.$$
$$\left.+\frac{\partial \mathbf{v}_i}{\partial x_j}\left[\left(I-\Pi_{\mathrm{k}}^{0,\mathrm{E}}\right)\mathbf{v}_j\right]\,\Pi_{\mathrm{k}}^{0,\mathrm{E}}\,\mathbf{w}_i+\left[\left(I-\Pi_{k-1}^{0,E}\right)\frac{\partial \mathbf{v}_i}{\partial x_j}\right]\left(\Pi_{\mathrm{k}}^{0,\mathrm{E}}\,\mathbf{v}_j\right)\Pi_{\mathrm{k}}^{0,\mathrm{E}}\,\mathbf{w}_i\right)\,\mathrm{d}E$$
$$=:\sum_{E\in\Omega_h}\sum_{i,j=1}^{2}\int_E(\alpha(\mathbf{w})+\beta(\mathbf{w})+\gamma(\mathbf{w}))\,\mathrm{d}E.$$

Now, by definition of L^2-projection $\Pi_{\mathrm{k}}^{0,\mathrm{E}}$ and by Lemma 4.2, we have

(72)
$$\begin{aligned}\int_E\alpha(\mathbf{w})\,\mathrm{d}E&=\int_E\frac{\partial \mathbf{v}_i}{\partial x_j}\,\mathbf{v}_j\left[\left(I-\Pi_{\mathrm{k}}^{0,\mathrm{E}}\right)\mathbf{w}_i\right]\mathrm{d}E\\&=\int_E\left[\left(I-\Pi_{k-2}^{0,E}\right)\left(\frac{\partial \mathbf{v}_i}{\partial x_j}\,\mathbf{v}_j\right)\right]\left[\left(I-\Pi_{\mathrm{k}}^{0,\mathrm{E}}\right)\mathbf{w}_i\right]\mathrm{d}E\\&\le\left\|\left(I-\Pi_{k-2}^{0,E}\right)\left(\frac{\partial \mathbf{v}_i}{\partial x_j}\,\mathbf{v}_j\right)\right\|_{0,E}\left\|\left(I-\Pi_{\mathrm{k}}^{0,\mathrm{E}}\right)\mathbf{w}_i\right\|_{0,E}\\&\le C\,h_E^s\left|\frac{\partial \mathbf{v}_i}{\partial x_j}\,\mathbf{v}_j\right|_{s-1,E}|\mathbf{w}_i|_{1,E}.\end{aligned}$$

Applying the Hölder inequality (for sequences), we get

(73)
$$\begin{aligned}\sum_{E\in\Omega_h}\sum_{i,j=1}^{2}\int_E\alpha(\mathbf{w})\,\mathrm{d}E&\le C\,h^s\sum_{E\in\Omega_h}\sum_{i,j=1}^{2}\left|\frac{\partial \mathbf{v}_i}{\partial x_j}\,\mathbf{v}_j\right|_{s-1,E}|\mathbf{w}_i|_{1,E}\\&\le C\,h^s\sum_{i,j=1}^{2}\left(\sum_{E\in\Omega_h}\left|\frac{\partial \mathbf{v}_i}{\partial x_j}\,\mathbf{v}_j\right|_{s-1,E}^2\right)^{\frac12}\left(\sum_{E\in\Omega_h}|\mathbf{w}_i|_{1,E}^2\right)^{\frac12}\\&\le C\,h^s\sum_{i,j=1}^{2}\left|\frac{\partial \mathbf{v}_i}{\partial x_j}\,\mathbf{v}_j\right|_{s-1}|\mathbf{w}_i|_1,\end{aligned}$$

and by the Hölder inequality and Sobolev embedding $H^s(\Omega)\subset W_4^{s-1}(\Omega)$, we infer

(74)
$$\left|\frac{\partial \mathbf{v}_i}{\partial x_j}\,\mathbf{v}_j\right|_{s-1}\le\left\|\frac{\partial \mathbf{v}_i}{\partial x_j}\right\|_{W_4^{s-1}}\|\mathbf{v}_j\|_{W_4^{s-1}}\le C\left\|\frac{\partial \mathbf{v}_i}{\partial x_j}\right\|_s\|\mathbf{v}_j\|_s.$$

By (73) and (74) we finally obtain

(75)
$$\sum_{E\in\Omega_h}\sum_{i,j=1}^{2}\alpha(\mathbf{w})\le C\,h^s\,\|\mathbf{v}\|_{s+1}\,\|\mathbf{v}\|_s\,\|\mathbf{w}\|_{\mathbf{V}}.$$

For the term $\beta(\mathbf{w})$ in (71), using the Hölder inequality, we have

(76)
$$\begin{aligned}\int_E\beta(\mathbf{w})\,\mathrm{d}E&=\int_E\frac{\partial \mathbf{v}_i}{\partial x_j}\left[\left(I-\Pi_{\mathrm{k}}^{0,\mathrm{E}}\right)\mathbf{v}_j\right]\,\Pi_{\mathrm{k}}^{0,\mathrm{E}}\,\mathbf{w}_i\,\mathrm{d}E\\&\le\left\|\frac{\partial \mathbf{v}_i}{\partial x_j}\right\|_{0,E}\left\|\left(I-\Pi_{\mathrm{k}}^{0,\mathrm{E}}\right)\mathbf{v}_j\right\|_{L^4(E)}\left\|\Pi_{\mathrm{k}}^{0,\mathrm{E}}\,\mathbf{w}_i\right\|_{L^4(E)}.\end{aligned}$$

Lemma 4.2 yields the existence of a polynomial $\mathbf{v}_{j,\pi} \in \mathbb{P}_k(E)$ such that

$$\|\mathbf{v}_j - \mathbf{v}_{j,\pi}\|_{L^4(E)} \leq C\, h_E^s\, |\mathbf{v}_j|_{W_4^s(E)},$$

and thus, by the continuity of $\Pi_{\mathrm{k}}^{0,\mathrm{E}}$ with respect to the L^4-norm (cf. (35)),

$$\begin{aligned} \left\| \left(I - \Pi_{\mathrm{k}}^{0,\mathrm{E}} \right) \mathbf{v}_j \right\|_{L^4(E)} &\leq \|\mathbf{v}_j - \mathbf{v}_{j,\pi}\|_{L^4(E)} + \left\| \Pi_{\mathrm{k}}^{0,\mathrm{E}} \left(\mathbf{v}_j - \mathbf{v}_{j,\pi} \right) \right\|_{L^4(E)} \\ &\leq C \|\mathbf{v}_j - \mathbf{v}_{j,\pi}\|_{L^4(E)} \leq C\, h_E^s\, |\mathbf{v}_j|_{W_4^s(E)}. \end{aligned} \tag{77}$$

Using again the continuity of $\Pi_{\mathrm{k}}^{0,\mathrm{E}}$ with respect to the L^4-norm, by (76) and (77) we infer

$$\int_E \beta(\mathbf{w})\, \mathrm{d}E \leq C\, h_E^s \left\| \frac{\partial \mathbf{v}_i}{\partial x_j} \right\|_{0,E} |\mathbf{v}_j|_{W_4^s(E)}\, \|\mathbf{w}_i\|_{L^4(E)}.$$

Applying the Hölder inequality and Sobolev embeddings $H^1(\Omega) \subset L^4(\Omega)$ and $H^{s+1}(\Omega) \subset W_4^s(\Omega)$, we obtain

$$\begin{aligned} \sum_{E\in\Omega_h} \sum_{i,j=1}^{2} \int_E \beta(\mathbf{w})\, \mathrm{d}E &\leq C\, h^s \sum_{E\in\Omega_h} \sum_{i,j=1}^{2} \left\| \frac{\partial \mathbf{v}_i}{\partial x_j} \right\|_{0,E} |\mathbf{v}_j|_{W_4^s(E)}\, \|\mathbf{w}_i\|_{L^4(E)} \\ &\leq C\, h^s \sum_{i,j=1}^{2} \left(\sum_{E\in\Omega_h} \left\| \frac{\partial \mathbf{v}_i}{\partial x_j} \right\|_{0,E}^2 \right)^{\frac{1}{2}} \left(\sum_{E\in\Omega_h} |\mathbf{v}_j|_{W_4^s(E)}^4 \right)^{\frac{1}{4}} \left(\sum_{E\in\Omega_h} \|\mathbf{w}_i\|_{L^4(E)}^4 \right)^{\frac{1}{4}} \\ &\leq C\, h^s \sum_{i,j=1}^{2} \left\| \frac{\partial \mathbf{v}_i}{\partial x_j} \right\|_0 \|\mathbf{v}_j\|_{W_4^s}\, \|\mathbf{w}_i\|_{L^4} \leq C\, h^s\, \|\mathbf{v}\|_{\mathbf{V}}\, \|\mathbf{v}\|_{s+1}\, \|\mathbf{w}\|_{\mathbf{V}}. \end{aligned} \tag{78}$$

For the term $\gamma(\mathbf{w})$ in (71), using the Hölder inequality and the continuity of $\Pi_{\mathrm{k}}^{0,\mathrm{E}}$, it holds that

$$\begin{aligned} \int_E \gamma(\mathbf{w})\, \mathrm{d}E &= \int_E \left[\left(I - \Pi_{k-1}^{0,E} \right) \frac{\partial \mathbf{v}_i}{\partial x_j} \right] \left(\Pi_{\mathrm{k}}^{0,\mathrm{E}}\, \mathbf{v}_j \right) \Pi_{\mathrm{k}}^{0,\mathrm{E}}\, \mathbf{w}_i\, \mathrm{d}E \\ &\leq \left\| \left(I - \Pi_{k-1}^{0,E} \right) \frac{\partial \mathbf{v}_i}{\partial x_j} \right\|_{0,E} \|\, \Pi_{\mathrm{k}}^{0,\mathrm{E}}\, \mathbf{v}_j\|_{L^4(E)}\, \|\, \Pi_{\mathrm{k}}^{0,\mathrm{E}}\, \mathbf{w}_i\|_{L^4(E)} \\ &\leq C\, h_E^s \left| \frac{\partial \mathbf{v}_i}{\partial x_j} \right|_{s,E} \|\mathbf{v}_j\|_{L^4(E)}\, \|\mathbf{w}_i\|_{L^4(E)}. \end{aligned} \tag{79}$$

Using again the Hölder inequality and Sobolev embedding, we get

$$\sum_{E\in\Omega_h} \sum_{i,j=1}^{2} \int_E \gamma(\mathbf{w})\, \mathrm{d}E \leq C\, h^s\, \|\mathbf{v}\|_{\mathbf{V}}\, \|\mathbf{w}\|_{\mathbf{V}}\, \|\mathbf{v}\|_{s+1}. \tag{80}$$

By combining (75), (78), and (80) in (71) we finally get

$$\mu_1(\mathbf{w}) \leq C\, h^s\, \left(\|\mathbf{v}\|_{s+1} \|\mathbf{v}\|_s + \|\mathbf{v}\|_{s+1} \|\mathbf{v}\|_{\mathbf{V}} \right) \|\mathbf{w}\|_{\mathbf{V}}. \tag{81}$$

For the second term $\mu_2(\mathbf{w})$ we only sketch the proof since we use analogous arguments.

First by definition, then by adding and subtracting terms, we obtain

(82)
$$\begin{aligned}\mu_2(\mathbf{w}) = &\sum_{E\in\Omega_h}\sum_{i,j=1}^{2}\int_E \Bigg(\left[\left(I-\Pi^{0,E}_{k-1}\right)\frac{\partial \mathbf{w}_i}{\partial x_j}\right]\mathbf{v}_j\,\mathbf{v}_i + \left(\Pi^{0,E}_{k-1}\frac{\partial \mathbf{w}_i}{\partial x_j}\right)\left[\left(I-\Pi^{0,\mathrm{E}}_{\mathrm{k}}\right)\mathbf{v}_j\right]\mathbf{v}_i \\ &+\left(\Pi^{0,E}_{k-1}\frac{\partial \mathbf{w}_i}{\partial x_j}\right)\left(\Pi^{0,\mathrm{E}}_{\mathrm{k}}\,\mathbf{v}_j\right)\left[\left(I-\Pi^{0,\mathrm{E}}_{\mathrm{k}}\right)\mathbf{v}_i\right]\Bigg)\,\mathrm{d}E \\ =:&\sum_{E\in\Omega_h}\sum_{i,j=1}^{2}\int_E (\delta(\mathbf{w})+\varepsilon(\mathbf{w})+\zeta(\mathbf{w}))\,\mathrm{d}E.\end{aligned}$$

For the term $\delta(\mathbf{w})$ we have

(83)
$$\begin{aligned}\int_E \delta(\mathbf{w})\,\mathrm{d}E &= \int_E\left[\left(I-\Pi^{0,E}_{k-1}\right)\frac{\partial \mathbf{w}_i}{\partial x_j}\right]\mathbf{v}_j\,\mathbf{v}_i\,\mathrm{d}E \\ &= \int_E\left[\left(I-\Pi^{0,E}_{k-1}\right)\frac{\partial \mathbf{w}_i}{\partial x_j}\right]\left[\left(I-\Pi^{0,E}_{k-1}\right)\mathbf{v}_j\,\mathbf{v}_i\right]\mathrm{d}E \\ &\le \left\|\left(I-\Pi^{0,E}_{k-1}\right)\frac{\partial \mathbf{w}_i}{\partial x_j}\right\|_{0,E}\left\|\left(I-\Pi^{0,E}_{k-1}\right)\mathbf{v}_j\,\mathbf{v}_i\right\|_{0,E} \\ &\le C\sum_{i,j=1}^{2} h_E^s\left\|\frac{\partial \mathbf{w}_i}{\partial x_j}\right\|_{0,E}|\mathbf{v}_j\,\mathbf{v}_i|_{s,E},\end{aligned}$$

and applying the Hölder inequality (for sequences) we easily get

$$\sum_{E\in\Omega_h}\sum_{i,j=1}^{2}\int_E \delta(\mathbf{w})\,\mathrm{d}E \le C\,h^s\sum_{i,j=1}^{2}\left\|\frac{\partial \mathbf{w}_i}{\partial x_j}\right\|_0|\mathbf{v}_j\,\mathbf{v}_i|_s.$$

The Hölder inequality and the Sobolev embedding $H^{s+1}(\Omega)\subset W^s_4(\Omega)$ yield

$$|\mathbf{v}_j\,\mathbf{v}_i|_s \le \|\mathbf{v}_j\|_{W^s_4}\,\|\mathbf{v}_i\|_{W^s_4} \le C\,\|\mathbf{v}_j\|_{s+1}\,\|\mathbf{v}_i\|_{s+1},$$

and thus we conclude that

$$\sum_{E\in\Omega_h}\sum_{i,j=1}^{2}\delta(\mathbf{w}) \le C\,h^s\,\|\mathbf{v}\|^2_{s+1}\,\|\mathbf{w}\|_{\mathbf{V}}. \tag{84}$$

The terms $\varepsilon(\mathbf{w})$ and $\zeta(\mathbf{w})$ can be estimated using the usual argument (Hölder inequality, continuity of $\Pi^{0,\mathrm{E}}_{\mathrm{k}}$ with respect to the L^4-norm, and Sobolev embeddings). We conclude that

$$\mu_2(\mathbf{w}) \le C\,h^s\,\left(\|\mathbf{v}\|^2_{s+1}+\|\mathbf{v}\|_{s+1}\|\mathbf{v}\|_{\mathbf{V}}\right)\|\mathbf{w}\|_{\mathbf{V}}. \tag{85}$$

We infer the proof by combining (81) and (85) in (70). ∎

LEMMA 4.4. *Let $\widehat{C}_h$ be the constant defined in* (32)*. Then for all $\mathbf{v},\mathbf{z},\mathbf{w}\in\mathbf{V}$ it holds that*

$$|\widetilde{c}_h(\mathbf{v};\,\mathbf{v},\mathbf{w})-\widetilde{c}_h(\mathbf{z};\,\mathbf{z},\mathbf{w})| \le \widehat{C}_h\,\left(\|\mathbf{z}\|_{\mathbf{V}}\,\|\mathbf{w}\|_{\mathbf{V}}+\|\mathbf{v}-\mathbf{z}+\mathbf{w}\|_{\mathbf{V}}(\|\mathbf{v}\|_{\mathbf{V}}+\|\mathbf{z}\|_{\mathbf{V}})\right)\|\mathbf{w}\|_{\mathbf{V}}.$$

Proof. Since $\widetilde{c}_h(\cdot;\,\cdot,\cdot)$ is skew-symmetric, by simple computations we obtain

$$\begin{aligned}\widetilde{c}_h(\mathbf{v};\,\mathbf{v},\mathbf{w})-\widetilde{c}_h(\mathbf{z};\,\mathbf{z},\mathbf{w}) &= \widetilde{c}_h(\mathbf{v};\,\mathbf{v}-\mathbf{z},\mathbf{w})+\widetilde{c}_h(\mathbf{v}-\mathbf{z};\,\mathbf{z},\mathbf{w})\\ &= \widetilde{c}_h(\mathbf{v};\,\mathbf{v}-\mathbf{z}+\mathbf{w},\mathbf{w})+\widetilde{c}_h(\mathbf{v}-\mathbf{z}+\mathbf{w},\,\mathbf{z},\mathbf{w})-\widetilde{c}_h(\mathbf{w};\,\mathbf{z},\mathbf{w}).\end{aligned}$$

The proof follows by definitions (39) and (32). ∎

Furthermore, we state the following result concerning the load approximation, which can be proved using standard arguments [11].

LEMMA 4.5. *Let $\mathbf{f}_h$ be defined as in* (40)*, and let us assume $\mathbf{f}\in H^{s+1}(\Omega)$, $-1\le s\le k$. Then, for all $\mathbf{v}_h\in\mathbf{V}_h$, it holds that*

$$|(\mathbf{f}_h-\mathbf{f},\mathbf{v}_h)|\le Ch^{s+2}|\mathbf{f}|_{s+1}|\mathbf{v}_h|_{\mathbf{V}}.$$

We now note that, given $\mathbf{v}\in\mathbf{Z}$, the inf-sup condition (43) implies (see [20])

$$\inf_{\mathbf{v}_h\in\mathbf{Z}_h,\mathbf{v}_h\neq\mathbf{0}}\|\mathbf{v}-\mathbf{v}_h\|_{\mathbf{V}}\le C\inf_{\mathbf{w}_h\in\mathbf{V}_h,\mathbf{w}_h\neq\mathbf{0}}\|\mathbf{v}-\mathbf{w}_h\|_{\mathbf{V}},$$

which essentially means that $\mathbf{Z}$ is approximated by $\mathbf{Z}_h$ with the same accuracy order as the whole subspace $\mathbf{V}_h$. In particular by Theorem 4.1, assuming $\mathbf{v}\in H^{s+1}(\Omega)\cap\mathbf{Z}$, $0<s\le k$, we infer

$$\inf_{\mathbf{v}_h\in\mathbf{Z}_h,\mathbf{v}_h\neq\mathbf{0}}\|\mathbf{v}-\mathbf{v}_h\|_{\mathbf{V}}\le C\,h^s\,|\mathbf{v}|_{s+1}. \tag{86}$$

THEOREM 4.6. *Under assumptions* (9) *and* (44)*, let $\mathbf{u}$ be the solution of problem* (12) *and $\mathbf{u}_h$ be the solution of virtual problem* (47)*. Assuming, moreover, $\mathbf{u},\mathbf{f}\in[H^{s+1}(\Omega)]^2$, $0<s\le k$, then*

$$\|\mathbf{u}-\mathbf{u}_h\|_{\mathbf{V}}\le\ h^s\,\mathcal{F}(\mathbf{u};\,\nu,\gamma,\gamma_h)+\ h^{s+2}\,\mathcal{H}(\mathbf{f};\nu,\gamma_h), \tag{87}$$

where $\mathcal{F}$ and $\mathcal{H}$ are suitable functions independent of h.

Proof. Let $\mathbf{u}_I$ be an approximant of $\mathbf{u}$ in the discrete kernel $\mathbf{Z}_h$ satisfying (86), and let us define $\boldsymbol{\delta}_h:=\mathbf{u}_h-\mathbf{u}_I$. Now, by the stability and the consistency properties (cf. (27) and (28)) of the bilinear form $a_h(\cdot,\cdot)$, the triangular inequality and (86) give

(88)
$$\begin{aligned}\alpha_*\,\nu\,\|\boldsymbol{\delta}_h\|_{\mathbf{V}}^2 &\le \nu\,a_h(\boldsymbol{\delta}_h,\,\boldsymbol{\delta}_h)=\nu\,a_h(\mathbf{u}_h,\,\boldsymbol{\delta}_h)-\nu\,a_h(\mathbf{u}_I,\,\boldsymbol{\delta}_h)\\ &= \nu\,a_h(\mathbf{u}_h,\,\boldsymbol{\delta}_h)-\nu\,a(\mathbf{u},\,\boldsymbol{\delta}_h)+\nu\sum_{E\in\Omega_h}\big(a_h^E(\mathbf{u}_\pi-\mathbf{u}_I,\,\boldsymbol{\delta}_h)+a^E(\mathbf{u}-\mathbf{u}_\pi,\,\boldsymbol{\delta}_h)\big)\\ &\le \nu\,a_h(\mathbf{u}_h,\,\boldsymbol{\delta}_h)-\nu\,a(\mathbf{u},\,\boldsymbol{\delta}_h)+C\,\nu\,h^s|\mathbf{u}|_{s+1}\|\boldsymbol{\delta}_h\|_{\mathbf{V}},\end{aligned}$$

where $\mathbf{u}_\pi$ is the piecewise polynomial of degree k defined in Lemma 4.2. Now since $\mathbf{u}$ and $\mathbf{u}_h$ are solutions of problems (12) and (47), respectively, from Lemma 4.5 we obtain

$$\begin{aligned}\alpha_*\,\nu\,\|\boldsymbol{\delta}_h\|_{\mathbf{V}}^2 &\le (\mathbf{f}_h-\mathbf{f},\,\boldsymbol{\delta}_h)+\widetilde{c}(\mathbf{u};\,\mathbf{u},\boldsymbol{\delta}_h)-\widetilde{c}_h(\mathbf{u}_h;\,\mathbf{u}_h,\boldsymbol{\delta}_h)+C\,\nu\,h^s|\mathbf{u}|_{s+1}\|\boldsymbol{\delta}_h\|_{\mathbf{V}}\\ &\le C\,h^s(\nu\,|\mathbf{u}|_{s+1}+h^2\,|\mathbf{f}|_{s+1})\|\boldsymbol{\delta}_h\|_{\mathbf{V}}+\widetilde{c}(\mathbf{u};\,\mathbf{u},\boldsymbol{\delta}_h)-\widetilde{c}_h(\mathbf{u}_h;\,\mathbf{u}_h,\boldsymbol{\delta}_h).\end{aligned} \tag{89}$$

Now we observe that

(90)
$$\widetilde{c}(\mathbf{u};\,\mathbf{u},\boldsymbol{\delta}_h)-\widetilde{c}_h(\mathbf{u}_h;\,\mathbf{u}_h,\boldsymbol{\delta}_h)=\big(\widetilde{c}(\mathbf{u};\,\mathbf{u},\boldsymbol{\delta}_h)-\widetilde{c}_h(\mathbf{u};\,\mathbf{u},\boldsymbol{\delta}_h)\big)+\big(\widetilde{c}_h(\mathbf{u};\,\mathbf{u},\boldsymbol{\delta}_h)-\widetilde{c}_h(\mathbf{u}_h;\,\mathbf{u}_h,\boldsymbol{\delta}_h)\big).$$

The first term can be estimated by Lemma 4.3:

$$|\widetilde{c}(\mathbf{u};\,\mathbf{u},\boldsymbol{\delta}_h)-\widetilde{c}_h(\mathbf{u};\,\mathbf{u},\boldsymbol{\delta}_h)|\le C\,h^s\,\left(\|\mathbf{u}\|_s+\|\mathbf{u}\|_{\mathbf{V}}+\|\mathbf{u}\|_{s+1}\right)\|\mathbf{u}\|_{s+1}\,\|\boldsymbol{\delta}_h\|_{\mathbf{V}}.$$

The second term, recalling that $\boldsymbol{\delta}_h=\mathbf{u}_h-\mathbf{u}_I$, is bounded by Lemma 4.4:

(91)
$$|\widetilde{c}_h(\mathbf{u};\,\mathbf{u},\boldsymbol{\delta}_h)-\widetilde{c}_h(\mathbf{u}_h;\,\mathbf{u}_h,\boldsymbol{\delta}_h)|\le\widehat{C}_h\left(\|\mathbf{u}_h\|_{\mathbf{V}}\,\|\boldsymbol{\delta}_h\|_{\mathbf{V}}+\|\mathbf{u}-\mathbf{u}_I\|_{\mathbf{V}}(\|\mathbf{u}\|_{\mathbf{V}}+\|\mathbf{u}_h\|_{\mathbf{V}})\right)\|\boldsymbol{\delta}_h\|_{\mathbf{V}}.$$

Combining (90) and (91) in (89), we get

(92)
$$\begin{aligned}\alpha_*\,\nu\,\|\boldsymbol{\delta}_h\|_{\mathbf{V}}\le{}&C\,h^s(\nu\,|\mathbf{u}|_{s+1}+h^2\,|\mathbf{f}|_{s+1})+C\,h^s\,\left(\|\mathbf{u}\|_s+\|\mathbf{u}\|_{\mathbf{V}}+\|\mathbf{u}\|_{s+1}\right)\|\mathbf{u}\|_{s+1}\\&+\widehat{C}_h\left(\|\mathbf{u}_h\|_{\mathbf{V}}\,\|\boldsymbol{\delta}_h\|_{\mathbf{V}}+\|\mathbf{u}-\mathbf{u}_I\|_{\mathbf{V}}(\|\mathbf{u}\|_{\mathbf{V}}+\|\mathbf{u}_h\|_{\mathbf{V}})\right),\end{aligned}$$

and then by Theorem 4.1 we infer

$$\begin{aligned}(93)\quad&\alpha_*\,\nu\left(1-\frac{\widehat{C}_h\,\|\mathbf{u}_h\|_{\mathbf{V}}}{\alpha_*\,\nu}\right)\|\boldsymbol{\delta}_h\|_{\mathbf{V}}\le C\,h^s(\nu\,|\mathbf{u}|_{s+1}+h^2\,|\mathbf{f}|_{s+1})\\&+C\,h^s\,\left(\|\mathbf{u}\|_s+\|\mathbf{u}\|_{\mathbf{V}}+\|\mathbf{u}\|_{s+1}\right)\|\mathbf{u}\|_{s+1}+C\,h^s\,\|\mathbf{u}\|_{s+1}\,\widehat{C}_h\,(\|\mathbf{u}\|_{\mathbf{V}}+\|\mathbf{u}_h\|_{\mathbf{V}}).\end{aligned}$$

We observe now that from (45) and (44), it holds that

$$1-\frac{\widehat{C}_h\,\|\mathbf{u}_h\|_{\mathbf{V}}}{\alpha_*\,\nu}\ge1-\frac{\widehat{C}_h\,\|\mathbf{f}_h\|_{H^{-1}}}{(\alpha_*\,\nu)^2}\ge1-r>0.$$

Therefore

$$\begin{aligned}\|\boldsymbol{\delta}_h\|_{\mathbf{V}}\le{}&C\,\frac{h^s}{1-r}\left(|\mathbf{u}|_{s+1}+\frac{h^2}{\nu}\|\mathbf{f}\|_{s+1}\right)+C\,\frac{h^s}{\nu(1-r)}\,\left(\|\mathbf{u}\|_s+\|\mathbf{u}\|_{\mathbf{V}}+\|\mathbf{u}\|_{s+1}\right)\|\mathbf{u}\|_{s+1}\\&+C\,h^s\,\|\mathbf{u}\|_{s+1}\,\frac{\widehat{C}_h}{\nu(1-\gamma_h)}\,(\|\mathbf{u}\|_{\mathbf{V}}+\|\mathbf{u}_h\|_{\mathbf{V}}),\end{aligned}$$

and from (10), (9), (45), and (44) we finally obtain

$$\begin{aligned}\|\boldsymbol{\delta}_h\|_{\mathbf{V}}\le{}&C\,\frac{h^s}{1-r}\left(|\mathbf{u}|_{s+1}+\frac{h^2}{\nu}\|\mathbf{f}\|_{s+1}\right)+C\,\frac{h^s}{\nu(1-r)}\,\left(\|\mathbf{u}\|_s+\|\mathbf{u}\|_{\mathbf{V}}+\|\mathbf{u}\|_{s+1}\right)\|\mathbf{u}\|_{s+1}\\&+C\,h^s\,\|\mathbf{u}\|_{s+1}\,\left(\frac{\widehat{C}_h}{\widehat{C}}\,\frac{\gamma}{1-r}+\frac{\gamma_h}{1-r}\right).\end{aligned}$$

The proof easily follows from the triangular inequality. ∎

Remark 4.1. We observe that, due to the divergence-free property of the proposed method, the estimate on the velocity errors in Theorem 4.6 does not depend on the continuous pressure, whereas the velocity errors of classical methods have a pressure contribution. A numerical investigation of this aspect, also in relation to the presence of a higher order load approximation term in the right-hand side of (87), will be shown in the next section.

Remark 4.2. From the discrete inf-sup condition (43) the pressure estimate easily follows by standard arguments. Let $(\mathbf{u}, p) \in \mathbf{V} \times Q$ be the solution of problem (7) and $(\mathbf{u}_h, p_h) \in \mathbf{V}_h \times Q_h$ be the solution of problem (42). Then it holds that

$$\|p - p_h\|_Q \leq C\, h^s\, |p|_s + C\, h^{s+2}\, |\mathbf{f}|_{s+1} + h^s\, \mathcal{K}(\mathbf{u}; \nu, \gamma, \gamma_h) \tag{94}$$

for a suitable function $\mathcal{K}(\cdot;\, \cdot, \cdot)$ independent of h.

Remark 4.3. In Theorem 4.6 we have assumed $\mathbf{u}$ and $\mathbf{f}$ in $H^{s+1}(\Omega)$. However, it is easy to check that the same analysis can be performed if we only require

$$\mathbf{u},\, \mathbf{f} \in H^{s+1}(E) \quad \text{for all } E \in \Omega_h.$$

In such a case, the higher order Sobolev norms on $\mathbf{u}, \mathbf{f}$ appearing in Theorem 4.6 (and in the other results of this section) are replaced by the corresponding elementwise broken Sobolev norms.

5. Numerical tests. In this section we present six sets of numerical experiments to test the practical performance of the method. All of the tests are performed with the second order VEM, i.e., $k = 2$. We also consider suitable second order finite elements for comparison. In almost all cases, both options $c_h(\cdot;\, \cdot, \cdot)$ and $\widetilde{c}_h(\cdot;\, \cdot, \cdot)$ (see Remark 3.5) yield very similar results; in such cases, only the first choice is reported. However, whenever the results between the two choices are significantly different, both outcomes are shown.

In Tests 5.1 and 5.2, we consider two benchmark problems for the Stokes and Navier–Stokes equations. They share the property of having the velocity solution in the discrete space. However, classical mixed finite element methods lead to significant velocity errors, stemming from the velocity-pressure coupling in the error estimates. This effect is greatly reduced (or even absent) with our VEMs (cf. Theorem 4.6 and estimate (94)). In Test 5.3 we analyze the stability of the method with respect to the viscosity parameter ν. In Tests 5.4 and 5.5 we study the convergence of the proposed method for the Navier–Stokes and Stokes equations, respectively. A comparison with the triangular P2-P1 and the quadrilateral Q2-P1 mixed finite element methods (see, for example, [20]), is also performed. Finally in Test 5.6 we assess the proposed VEM for flows which are governed by the Stokes system on one part of the domain and by the Darcy's law in the rest of the domain, the solutions in the two domains being coupled by proper interface conditions (see Remark 3.6).

In order to compute the VEM errors, we consider the computable error quantities:

$$\begin{aligned}
\text{error}(\mathbf{u}, H^1) &:= \left(\sum_{E \in \Omega_h} \left\| \boldsymbol{\nabla}\, \mathbf{u} - \boldsymbol{\Pi}^{0,E}_{k-1}(\boldsymbol{\nabla}\, \mathbf{u}_h) \right\|^2_{0,E} \right)^{1/2}, \\
\text{error}(\mathbf{u}, L^2) &:= \left(\sum_{E \in \Omega_h} \left\| \mathbf{u} - \Pi^{0,E}_k\, \mathbf{u}_h \right\|^2_{0,E} \right)^{1/2}, \\
\text{error}(\mathbf{u}, L^\infty) &:= \max_{\mathbf{x} \in \text{ nodes}} |\mathbf{u}(\mathbf{x}) - \mathbf{u}_h(\mathbf{x})|,
\end{aligned}$$

where in the previous formula "nodes" denotes the set of internal edge nodes and internal vertexes (cf. $\mathbf{D_V 1}$ and $\mathbf{D_V 2}$). For the pressures we simply compute

$$\text{error}(p, L^2) := \|p - p_h\|_0.$$

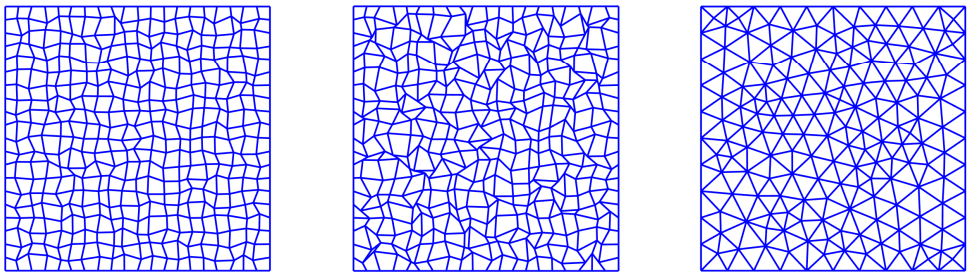

FIG. 2. *Example of the adopted polygonal meshes:* $\mathcal{Q}_{1/20}$, $\mathcal{U}_{1/20}$, *and* $\mathcal{T}_{1/10}$.

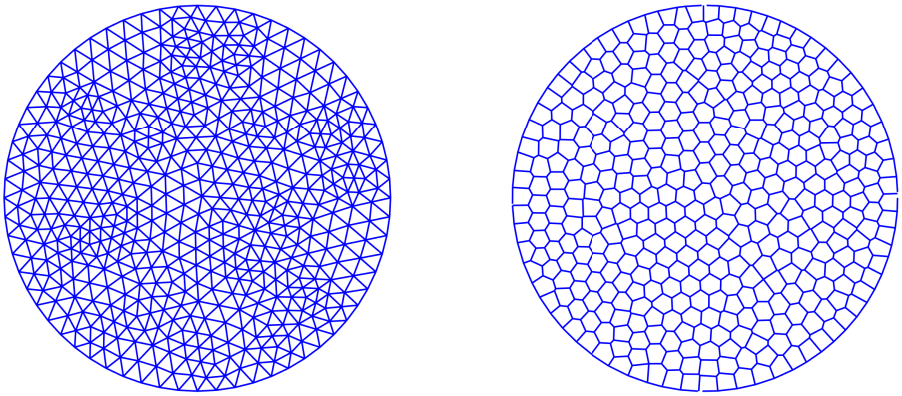

FIG. 3. *Example of polygonal meshes:* $\mathcal{S}_{1/10}$ *and* $\mathcal{V}_{1/10}$.

The polynomial degree of accuracy for the numerical tests is $k = 2$. In the experiments we consider the computational domains $\Omega_{\mathrm{Q}} := [0,1]^2$ and $\Omega_{\mathrm{D}} := \{\mathbf{x} \in \mathbb{R}^2 \,\text{s.t.}\, |\mathbf{x}| \leq 1\}$. The square domain Ω_{Q} is partitioned using the following sequences of polygonal meshes:

- $\{\mathcal{Q}_h\}_h$: distorted quadrilateral meshes with $h = 1/10, 1/20, 1/40, 1/80$,
- $\{\mathcal{U}_h\}_h$: distorted quadrilateral meshes with $h = 1/10, 1/20, 1/40, 1/80$,
- $\{\mathcal{T}_h\}_h$: triangular meshes with $h = 1/5, 1/10, 1/20, 1/40$.

An example of the adopted meshes is shown in Figure 2. The distorted quadrilateral meshes are obtained starting from the uniform square meshes and displacing the internal vertexes (with a proportional "distortion amplitude" of 0.3 for $\mathcal{Q}_h$ and 0.5 for $\mathcal{U}_h$). The nonconvex WEB-like meshes are composed by hexagons, generated starting from the triangular meshes $\{\mathcal{T}_h\}_h$ and randomly displacing the midpoint of each (nonboundary) edge. For what concerns the disk Ω_{D} we consider the sequences of polygonal meshes:

- $\{\mathcal{S}_h\}_h$: sequence of triangular meshes with $h = 1/5, 1/10, 1/20, 1/40$,
- $\{\mathcal{V}_h\}_h$: sequence of centroidal Voronoi meshes with $h = 1/5, 1/10, 1/20, 1/40$.

Figure 3 displays an example of the adopted meshes. For the generation of the Voronoi meshes we use the code Polymesher [50].

Remark 5.1. As a comparison, we make use also of the classical Q2-P1 and P2-P1 mixed finite elements; see for instance [20]. The Q2-P1 (Crousiex–Raviart) is a

quadrilateral element with biquadratic velocities and $\mathbb{P}_1$ discontinuous pressures. The P2-P1 (Taylor–Hood) is a triangular element with $\mathbb{P}_2$ velocities and $\mathbb{P}_1$ continuous pressures. Both are inf-sup stable elements, widely used in the literature and yielding a quadratic convergence rate in the natural norms of the problem.

Test 5.1 (hydrostatic fluids). In this test we consider the linear Stokes equation on the domain Ω_{Q} with external load $\mathbf{f} = \nabla p$ that exactly balances the gradient of the pressure, yielding a hydrostatic situation, i.e., $\mathbf{u} = \mathbf{0}$. We set the viscosity $\nu = 1$, and we consider two possible pressures,

$$p_1(x, y) = x^3 - y^3 \qquad \text{and} \qquad p_2(x, y) = \sin(2\pi x)\sin(2\pi y).$$

It is well known that the velocity error between the exact velocity $\mathbf{u}$ and the discrete velocity $\mathbf{u}_h$ of standard mixed elements like the Q2-P1 element for the incompressible Stokes equations is pressure-dependent, i.e., has the form

$$\|\mathbf{u} - \mathbf{u}_h\|_{\mathbf{V}} \leq C_1 \inf_{\mathbf{v}_h \mathbf{V}_h} \|\mathbf{u} - \mathbf{v}_h\|_{\mathbf{V}} + C_2 \inf_{q_h \in Q_h} \|p - q_h\|_Q, \tag{95}$$

where C_1, C_2 are two positive uniform constants, whereas for the virtual element scheme (see Theorem 4.6 and [15]) the error on the velocity does not depend on the pressure, i.e.,

$$\|\mathbf{u} - \mathbf{u}_h\|_{\mathbf{V}} \leq C_1 \inf_{\mathbf{v}_h \mathbf{V}_h} \|\mathbf{u} - \mathbf{v}_h\|_{\mathbf{V}} + C_2\, h^{k+2} |\mathbf{f}|_{k+1}. \tag{96}$$

We observe that for both VEM and Q2-P1, the pressures p_1 and p_2 do not belong to the discrete pressure space. Therefore we expect that the discrete Q2-P1 velocities are polluted by the pressure approximation. Table 1 shows the results obtained respectively with VEM and Q2-P1 for the case of polynomial pressure p_1 and sequence of meshes $\mathcal{Q}_h$. We observe that the VEM yields an exact hydrostatic velocity solution, since $\mathbf{f}$ is a polynomial of degree two, while the Q2-P1 finite element method, in accordance with the a priori estimate (95), shows nonnegligible errors in the velocity.

TABLE 1
Test 5.1*: Errors with VEM and Q2-P1 for polynomial pressure* p_1 *and meshes* $\mathcal{Q}_h$*.*

	h	error$(\mathbf{u}, H^1)$	error$(\mathbf{u}, L^2)$	error(p, L^2)
VEM	1/10	$7.157458e-16$	$2.565404e-17$	$2.117754e-03$
	1/20	$1.524395e-15$	$2.597817e-17$	$5.489919e-04$
	1/40	$1.610876e-15$	$1.589614e-17$	$1.377769e-04$
	1/80	$9.630624e-15$	$4.590908e-17$	$3.465069e-05$
Q2-P1	1/10	$5.328708e-04$	$9.142870e-06$	$8.202921e-03$
	1/20	$1.486154e-04$	$1.278884e-06$	$2.623095e-03$
	1/40	$4.105136e-05$	$1.737273e-07$	$3.433991e-04$
	1/80	$1.006121e-05$	$2.164782e-08$	$8.511695e-05$

On the other hand, we note that, due to the load approximation procedure, there is a load-dependent term in the right-hand side of (96). As a consequence, in the test with goniometric pressure p_2 (where the load $\mathbf{f}$ is not a polynomial), we expect a slight pollution of the velocity errors also for the VEM scheme, although much smaller than for the finite element method case. In Figure 4 we plot the errors for the goniometric pressure p_2 and the same sequence of meshes $\mathcal{Q}_h$. In accordance with the a priori estimates (95), (96) and the above observation, we obtain a quadratic convergence rate for the Q2-P1 finite element method, and a fourth order convergence rate for the VEM scheme for the H^1-velocity (quadratic for the L^2-pressure errors).

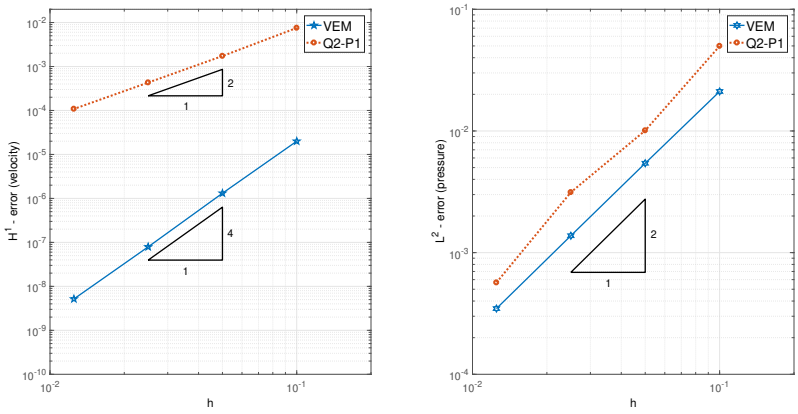

FIG. 4. *Test* 5.1: *Errors with VEM and* $Q2$-$P1$ *for the meshes* $\mathcal{Q}_h$.

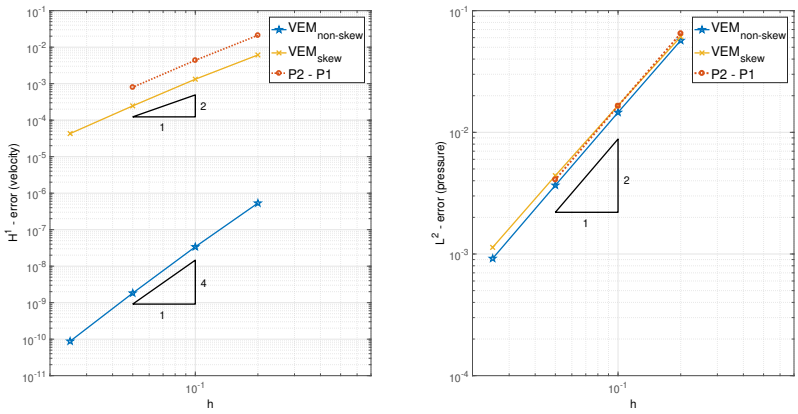

FIG. 5. *Test* 5.2: *Errors with VEM and* $P2$-$P1$ *with solution* $(\mathbf{u}, p)$ *and meshes* $\mathcal{S}_h$.

Test 5.2 (vanishing external load). In this test we consider a benchmark Navier–Stokes problem taken from [40] on the disk Ω_{D}, where we compare the results obtained with VEM discretization with those obtained with the standard P2-P1 element for the sequence of meshes $\mathcal{S}_h$. The solution is chosen in such a way that the pressure balances the nonlinear convective term, yielding a vanishing external load $\mathbf{f} = \mathbf{0}$. We take $\nu = 1$ and the exact solution

$$\mathbf{u}(x,y) = 3\begin{pmatrix} x^2 - y^2 \\ -2xy \end{pmatrix}, \qquad p(x,y) = 9\frac{(x^2+y^2)^2}{2} - \frac{3}{2}.$$

We notice that the velocity $\mathbf{u}$ belongs to the discrete space for both the VEM and P2-P1 schemes, whereas the pressure p does not. In Figure 5 we show the results obtained with the P2-P1 element and the VEM discretization, in which we use respectively the trilinear form $c_h(\cdot;\cdot,\cdot)$ of (31), labelled as $\mathrm{VEM}_{\text{non-skew}}$, and the skew-symmetric form $\widetilde{c}_h(\cdot;\cdot,\cdot)$ of (39), labelled as $\mathrm{VEM}_{\text{skew}}$ (cf. Remark 3.5). We observe that $\mathrm{VEM}_{\text{non-skew}}$ provides a better performance than both P2-P1 and $\mathrm{VEM}_{\text{skew}}$. Indeed, in this case it

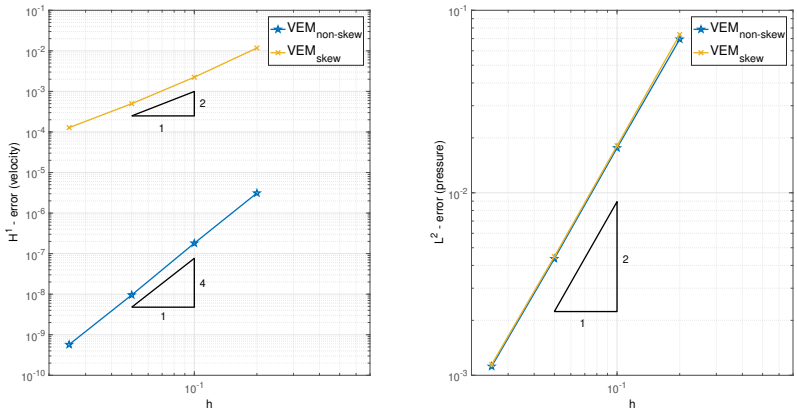

FIG. 6. *Test* 5.2: *Errors with VEM with solution* $(\mathbf{u}, p)$ *and meshes* $\mathcal{V}_h$.

holds that

$$|c_h(\mathbf{u};\,\mathbf{u},\mathbf{v}_h) - c(\mathbf{u};\,\mathbf{u},\mathbf{v}_h)| \leq C\,h^{k+2}|(\boldsymbol{\nabla}\mathbf{u})\,\mathbf{u}|_{k+1}||\mathbf{v}_h||_{\mathbf{V}} \qquad \text{for all } \mathbf{v}_h \in \mathbf{V}_h,$$

and using steps similar to those in the proof of Theorem 4.6, for $\text{VEM}_{\text{non-skew}}$ we can derive

$$\|\mathbf{u} - \mathbf{u}_h\|_{\mathbf{V}} \leq C\,h^{k+2}\,\|(\boldsymbol{\nabla}\mathbf{u}_2)\,\mathbf{u}\|_{k+1}.$$

Instead, for VEM_{skew} we can only obtain

$$\|\mathbf{u} - \mathbf{u}_h\|_{\mathbf{V}} \leq C\,h^{k}\,|\mathbf{u}\cdot\mathbf{u}|_{k}.$$

Finally, Figure 6 displays the results obtained with $\text{VEM}_{\text{non-skew}}$ and VEM_{skew} for the sequence of polygonal meshes $\mathcal{V}_h$ (see Figure 3). We refer the reader to [16] for a similar benchmark Navier–Stokes problem.

Test 5.3. In this example we test the Navier–Stokes equation on the domain Ω_{Q} with different values of the fluid viscosity ν. We choose the load term $\mathbf{f}$ in such a way that the analytical solution is

$$\mathbf{u}(x,y) = 0.1\begin{pmatrix} x^2(1-x)^2\,(2y-6y^2+4y^3) \\ -y^2(1-y)^2\,(2x-6x^2+4x^3)\end{pmatrix}, \qquad p(x,y) = x^3\,y^3 - \frac{1}{16}.$$

The aim of this test is to check the actual performance of the VEM for small viscosity parameters, in comparison with the standard P2-P1 mixed finite element method. Figure 7 shows that the solutions of the VEM are accurate even for rather small values of ν. Larger velocity errors appear only for very small viscosity parameters. The reason for this robustness is again that the "divergence-free" property of VEM yields velocity errors that do not depend directly on the pressure (but only indirectly through the higher order load approximation term; see Theorem 4.6). On the contrary, for the P2-P1 element the pressure component of the error can become the dominant source of error also for the velocity field. In addition, we note that for $\nu = 10^{-4}, 10^{-5}$ the P2-P1 element does not even converge.

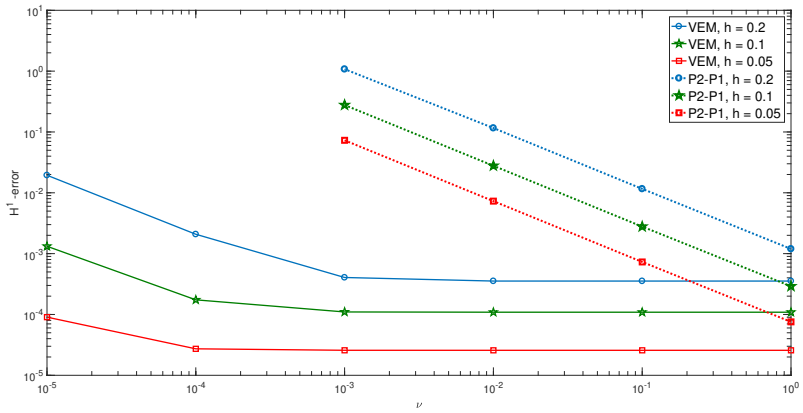

FIG. 7. *Test* 5.3: *Errors of VEM (dotted lines) and P2-P1 (solid lines), with different values of* ν *for the meshes* $\mathcal{T}_h$.

Test 5.4. In this test we solve the Navier–Stokes equation on the square domain Ω_Q with viscosity $\nu = 0.1$ and with the load term $\mathbf{f}$ chosen such that the analytical solution is

$$\mathbf{u}(x,y) = \frac{1}{2}\begin{pmatrix} \sin(2\pi x)^2 \sin(2\pi y)\cos(2\pi y) \\ -\sin(2\pi y)^2 \sin(2\pi x)\cos(2\pi x) \end{pmatrix}, \qquad p(x,y) = \pi^2 \sin(2\pi x)\cos(2\pi y).$$

In Figure 8 we show the results obtained for the sequence of triangular meshes $\mathcal{T}_h$, also compared with the P2-P1 element.

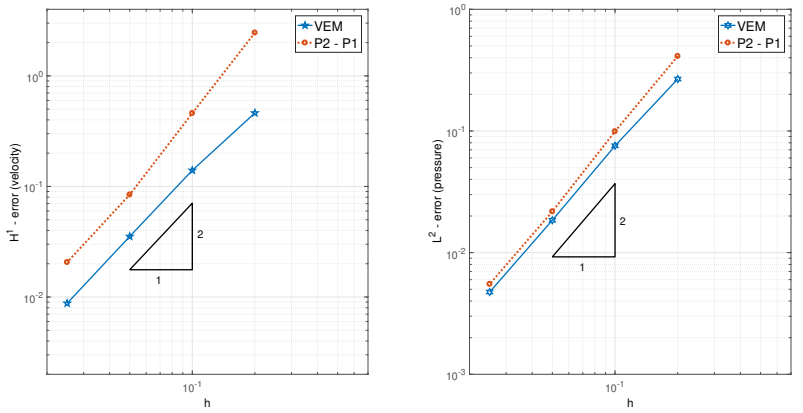

FIG. 8. *Test* 5.4: *Errors with VEM and P2-P1 for the meshes* $\mathcal{T}_h$.

We notice that the theoretical predictions of section 4 are confirmed. Moreover, we observe that the VEM exhibits smaller errors than the standard P2-P1 method, at least for this example and with the adopted meshes. We have tested the VEM also with a sequence of WEB-like polygonal meshes, obtaining that the theoretical predictions are confirmed as well. We refer the reader to the preprint [16] for the corresponding numerical results.

Test 5.5. In this experiment we analyze the Stokes equation on the square domain Ω_Q where the viscosity $\nu = 1$ and the load term $\mathbf{f}$ is chosen such that the analytical solution is

$$\mathbf{u}(x,y) = \frac{1}{2}\begin{pmatrix} \sin(2\pi x)^2 \sin(2\pi y)\cos(2\pi y) \\ -\sin(2\pi y)^2 \sin(2\pi x)\cos(2\pi x) \end{pmatrix}, \qquad p(x,y) = \sin(2\pi x)\cos(2\pi y).$$

The aim of this test is the assessment of the VEM robustness with respect to the mesh deformation, as well as a comparison with the Q2-P1 mixed finite element method. In Figure 9 we plot the obtained results.

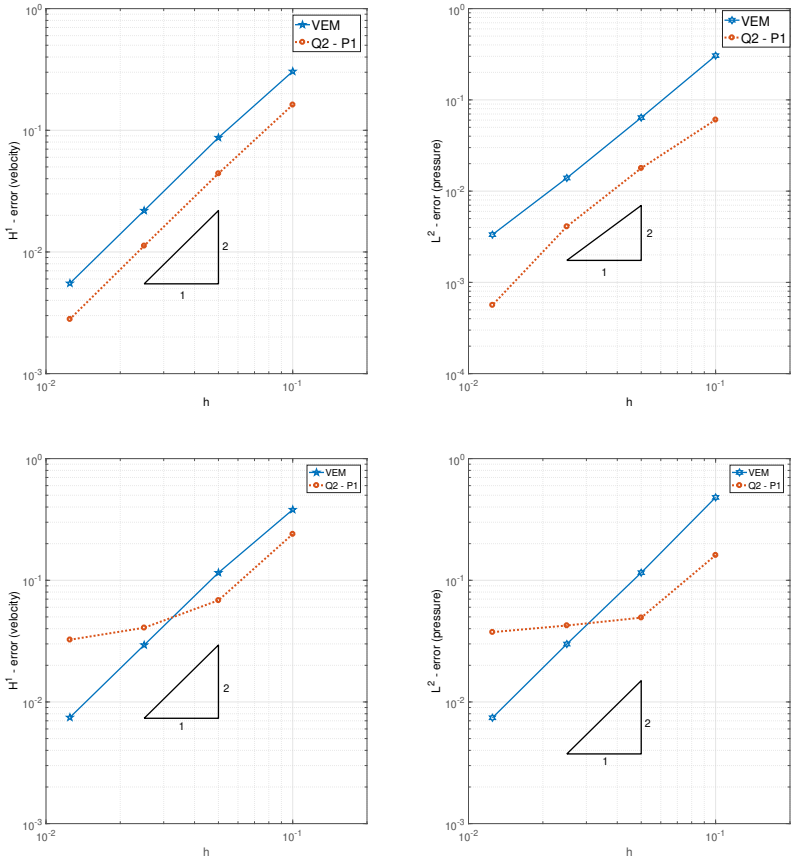

FIG. 9. *Test* 5.5: *Errors with VEM and Q2-P1 for the meshes* $\mathcal{Q}_h$ *(up) and* $\mathcal{U}_h$ *(down).*

We observe that for the (less deformed) quadrilateral meshes $\mathcal{Q}_h$, both the VEM and the Q2-P1 preserve the theoretical order of accuracy, but the Q2-P1 element yields better results. The overperformance is probably the effect of the tensor-product structure of this particular problem, which is not yet spoiled by the weak mesh distortion. Instead, for the (more deformed) sequence of meshes $\mathcal{U}_h$, the behavior is completely different. The virtual element approach maintains the optimal second order accuracy, whereas the Q2-P1 element clearly suffers from an evident suboptimality of the convergence rates (the pressure does not even seem to converge). Therefore, we may

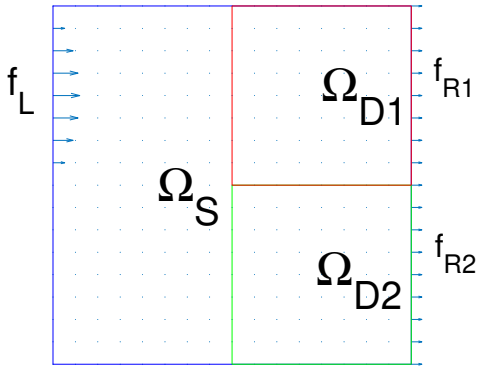

FIG. 10. *Test* 5.6: *The domain configuration of problem* (97).

conclude that the VEM seems to be more robust with respect to large distortions of the mesh.

Test 5.6. This test highlights that, following along the lines of [15, 52], the proposed virtual elements can accommodate both the Stokes (or Navier–Stokes) and the Darcy problems simultaneously (see Remark 3.6). Accordingly, we consider the approximation of a flow in the square $[0,2]^2$, consisting of a porous region $\Omega_D := \Omega_{D1} \cup \Omega_{D2}$, where the flow is a Darcy flow, and an open region $\Omega_S = \Omega \setminus \Omega_D$, where the flow is governed by the linear Stokes system (see Figure 10 for a depiction of the problem configuration). This leads us to consider the following problem: find $(\mathbf{u}, p) \in [H^1(\Omega)]^2 \times L^2(\Omega)$ such that

(97)
$$\begin{cases} -2\nu \operatorname{div}(\varepsilon(\mathbf{u})) - \nabla p = \mathbf{0} & \text{in } \Omega_S, \\ \operatorname{div} \mathbf{u} = 0 & \text{in } \Omega_S, \\ \mathbf{u}_1 = \varphi & \text{on } \{0\} \times [0,2], \\ \mathbf{u}_2 = 0 & \text{on } [0,1] \times \{0,2\}, \end{cases} \qquad \begin{cases} \nu\,\lambda \mathbf{u} - \nabla p = \mathbf{0} & \text{in } \Omega_D, \\ \operatorname{div} \mathbf{u} = 0 & \text{in } \Omega_D, \\ \mathbf{u}_2 = 0 & \text{on } [1,2] \times \{0,2\}, \end{cases}$$

where $\varepsilon(\mathbf{u}) := \frac{1}{2}(\boldsymbol{\nabla}\mathbf{u} + \boldsymbol{\nabla}\mathbf{u}^T)$ denotes the symmetric gradient operator. We fix $\nu = 1$, $\lambda = 10$ on Ω_{D1}, and $\lambda = 2$ on Ω_{D2}. Furthermore, we take

$$\varphi(0,y) = \max\{0, -10(1-y)(2-y)\}.$$

At the interface between the Stokes and Darcy regions, the system (97) is coupled using the Beavers–Joseph–Saffmann condition (see [7, 48] for further details).

We observe that in our test problem, we set free boundary conditions on the right boundary edge of the Darcy region. To test the performance of the VEM, the unknown quantities are (see Figure 10)

$$f_{R1} := \int_{\partial\Omega \cap \partial\Omega_{D1}} \mathbf{u} \cdot \mathbf{n}\, \mathrm{d}s \qquad \text{and} \qquad f_{R2} := \int_{\partial\Omega \cap \partial\Omega_{D2}} \mathbf{u} \cdot \mathbf{n}\, \mathrm{d}s,$$

taking into account that $f_L + f_{R1} + f_{R2} = 0$ and

$$f_L := \int_{\partial\Omega \cap \partial\Omega_S} \mathbf{u} \cdot \mathbf{n}\, \mathrm{d}s = -\frac{10}{6},$$

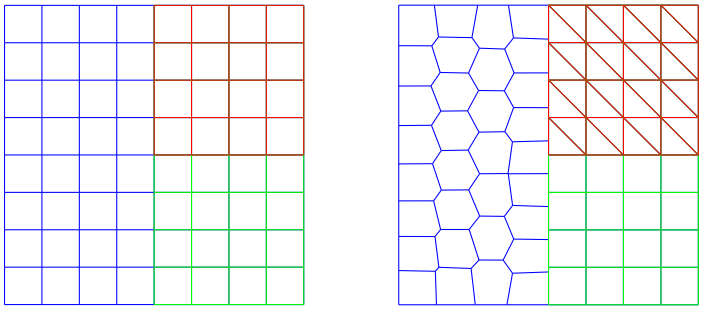

FIG. 11. *Test* 5.6: *Example of the adopted polygonal meshes* $\mathcal{Q}_{1/4}$ *(left) and* $\mathcal{P}_{1/4}$ *(right).*

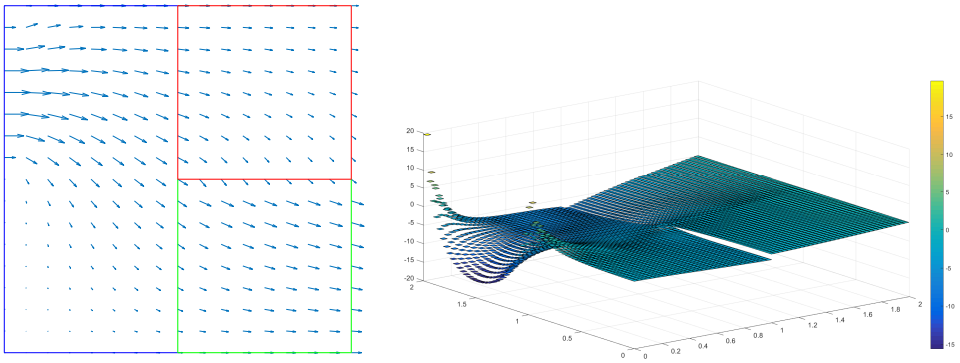

FIG. 12. *Test* 5.6: *Velocity and pressure respectively for the meshes* $\mathcal{Q}_{1/8}$ *and* $\mathcal{Q}_{1/32}$.

with $\mathbf{n}$ denoting the outward normal vector.

In this experiment the computational domain $\Omega := [0,2]^2$ is partitioned using two sequences of polygonal meshes:

- $\{\mathcal{Q}_h\}_h$: sequence of square meshes with element edge length $h = 1/4, 1/8, 1/16, 1/32$,
- $\{\mathcal{P}_h\}_h$: sequence of meshes obtained by gluing a Voronoi decomposition on the domain Ω_S, a triangular decomposition on Ω_{D1}, and a square decomposition on Ω_{D2}, with edge length $h = 1/4, 1/8, 1/16, 1/32$.

In addition, we use the square mesh $\mathcal{Q}_{1/64}$ as the basis for the reference solution. An example of the adopted meshes is shown in Figure 11. In Figure 12 we show the plot of the numerical velocity and pressure. Note that the purpose of mesh family $\{\mathcal{P}_h\}_h$ is to show the robustness of the proposed method when, by exploiting the flexibility of polygonal grids, completely independent meshes are glued together.

In Table 2 we show the results obtained by using the sequences of meshes $\mathcal{Q}_h$ and $\mathcal{P}_h$ compared with those obtained with the reference mesh. We observe that both sequences of meshes exhibit appropriate convergence properties, confirming that the proposed VEM can automatically handle nonconforming polygonal meshes and the coupling between Darcy and Stokes flow problems.

TABLE 2
Test 5.6: Fluxes along the boundary for the sequences of meshes $\mathcal{Q}_h$ and $\mathcal{P}_h$.

	h	f_{R1}	f_{R2}	$f_L + f_{R1} + f_{R2}$
Reference mesh	1/64	$5.373938e-01$	$1.129272e+00$	$-1.332267e-15$
$\mathcal{Q}_h$	1/4	$5.215469e-01$	$1.145119e+00$	0
	1/8	$5.284186e-01$	$1.138248e+00$	$4.440892e-16$
	1/16	$5.339269e-01$	$1.132739e+00$	$-4.44089e-16$
	1/32	$5.367736e-01$	$1.129893e+00$	$6.661338e-16$
$\mathcal{P}_h$	1/4	$5.161923e-01$	$1.158934e+00$	$4.440892e-16$
	1/8	$5.254995e-01$	$1.143962e+00$	$-4.44089e-16$
	1/16	$5.343364e-01$	$1.132836e+00$	$-2.22044e-16$
	1/32	$5.381031e-01$	$1.128622e+00$	0

REFERENCES

[1] B. AHMAD, A. ALSAEDI, F. BREZZI, L. D. MARINI, AND A. RUSSO, *Equivalent projectors for virtual element methods*, Comput. Math. Appl., 66 (2013), pp. 376–391.

[2] O. ANDERSEN, H. NILSEN, AND X. RAYNAUD, *Virtual element method for geomechanical simulations of reservoir models*, Comput. Geosci., 21 (2017), pp. 877–893.

[3] P. F. ANTONIETTI, L. BEIRÃO DA VEIGA, D. MORA, AND M. VERANI, *A stream virtual element formulation of the Stokes problem on polygonal meshes*, SIAM J. Numer. Anal., 52 (2014), pp. 386–404.

[4] E. ARTIOLI, L. BEIRÃO DA VEIGA, C. LOVADINA, AND E. SACCO, *Arbitrary order 2D virtual elements for polygonal meshes: Part* I*, elastic problem*, Comput. Mech., 60 (2017), pp. 355–377.

[5] E. ARTIOLI, S. DE MIRANDA, C. LOVADINA, AND L. PATRUNO, *A stress/displacement virtual element method for plane elasticity problems*, Comput. Methods Appl. Mech. Engrg., 325 (2017), pp. 155–174.

[6] B. AYUSO DE DIOS, K. LIPNIKOV, AND G. MANZINI, *The nonconforming virtual element method*, ESAIM Math. Model. Numer. Anal., 50 (2016), pp. 879–904.

[7] G. S. BEAVERS AND D. D. JOSEPH, *Boundary conditions at a naturally permeable wall*, J. Fluid Mech., 30 (1967), pp. 197–207.

[8] L. BEIRÃO DA VEIGA, F. BREZZI, AND L. D. MARINI, *Virtual elements for linear elasticity problems*, SIAM J. Numer. Anal., 51 (2013), pp. 794–812.

[9] L. BEIRÃO DA VEIGA, F. BREZZI, L. D. MARINI, AND A. RUSSO, *$H(\mathrm{div})$ and $H(\mathbf{curl})$-conforming virtual element methods*, Numer. Math., 133 (2016), pp. 303–332.

[10] L. BEIRÃO DA VEIGA, F. BREZZI, L. D. MARINI, AND A. RUSSO, *Virtual element methods for general second order elliptic problems on polygonal meshes*, Math. Models Methods Appl. Sci., 26 (2016), pp. 729–750.

[11] L. BEIRÃO DA VEIGA, F. BREZZI, A. CANGIANI, G. MANZINI, L. D. MARINI, AND A. RUSSO, *Basic principles of virtual element methods*, Math. Models Methods Appl. Sci., 23 (2013), pp. 199–214.

[12] L. BEIRÃO DA VEIGA, F. BREZZI, L. D. MARINI, AND A. RUSSO, *The hitchhiker's guide to the Virtual Element Method*, Math. Models Methods Appl. Sci., 24 (2014), pp. 1541–1573.

[13] L. BEIRÃO DA VEIGA, C. LOVADINA, AND D. MORA, *A virtual element method for elastic and inelastic problems on polytope meshes*, Comput. Methods Appl. Mech. Engrg., 295 (2015), pp. 327–346.

[14] L. BEIRÃO DA VEIGA, C. LOVADINA, AND A. RUSSO, *Stability analysis for the virtual element method*, Math. Models Methods Appl. Sci., 27 (2017), pp. 2557–2594.

[15] L. BEIRÃO DA VEIGA, C. LOVADINA, AND G. VACCA, *Divergence free virtual elements for the Stokes problem on polygonal meshes*, ESAIM Math. Model. Numer. Anal., 51 (2017), pp. 509–535.

[16] L. BEIRÃO DA VEIGA, C. LOVADINA, AND G. VACCA, *Virtual Elements for the Navier-Stokes Problem on Polygonal Meshes*, preprint, https://arxiv.org/abs/1703.00437, 2017.

[17] M. F. BENEDETTO, S. BERRONE, A. BORIO, S. PIERACCINI, AND S. SCIALÒ, *A hybrid mortar virtual element method for discrete fracture network simulations*, J. Comput. Phys., 306 (2016), pp. 148–166.

[18] M. F. Benedetto, S. Berrone, A. Borio, S. Pieraccini, and S. Scialò, *Order preserving SUPG stabilization for the virtual element formulation of advection–diffusion problems*, Comput. Methods Appl. Mech. Engrg., 311 (2016), pp. 18–40.
[19] M. F. Benedetto, S. Berrone, S. Pieraccini, and S. Scialò, *The Virtual Element Method for Discrete Fracture Network simulations*, Comput. Methods Appl. Mech. Engrg., 280 (2014), pp. 135–156.
[20] D. Boffi, F. Brezzi, and M. Fortin, *Mixed Finite Element Methods and Applications*, Springer Ser. Comput. Math. 44, Springer, Heidelberg, 2013.
[21] S. C. Brenner, Q. Guan, and L. Sung, *Some estimates for virtual element methods*, Comput. Methods Appl. Math., 17 (2017), pp. 553–574.
[22] S. C. Brenner and L. R. Scott, *The Mathematical Theory of Finite Element Methods*, 3rd ed., Texts Appl. Math. 15, Springer, New York, 2008.
[23] F. Brezzi, R. S. Falk, and L. D. Marini, *Basic principles of mixed virtual element methods*, ESAIM Math. Model. Numer. Anal., 48 (2014), pp. 1227–1240.
[24] F. Brezzi and L. D. Marini, *Virtual Element Methods for plate bending problems*, Comput. Methods Appl. Mech. Engrg., 253 (2013), pp. 455–462.
[25] E. Cáceres and G. N. Gatica, *A mixed virtual element method for the pseudostress-velocity formulation of the Stokes problem*, IMA J. Numer. Anal., 37 (2017), pp. 296–331.
[26] E. Cáceres, G. N. Gatica, and F. A. Sequeira, *A mixed virtual element method for the Brinkman problem*, Math. Models Methods Appl. Sci., 27 (2017), pp. 707–743.
[27] A. Cangiani, E. H. Georgoulis, T. Pryer, and O. J. Sutton, *A posteriori error estimates for the virtual element method*, Numer. Math., 137 (2017), pp. 857–893.
[28] A. Cangiani, V. Gyrya, and G. Manzini, *The nonconforming virtual element method for the Stokes equations*, SIAM J. Numer. Anal., 54 (2016), pp. 3411–3435.
[29] A. Cangiani, G. Manzini, and O. J. Sutton, *Conforming and nonconforming virtual element methods for elliptic problems*, IMA J. Numer. Anal., 37 (2017), pp. 1317–1354.
[30] H. Chi, L. Beirão da Veiga, and G. H. Paulino, *Some basic formulations of the virtual element method (VEM) for finite deformations*, Comput. Methods Appl. Mech. Engrg., 318 (2017), pp. 148–192.
[31] E. B. Chin, J. B. Lasserre, and N. Sukumar, *Numerical integration of homogeneous functions on convex and nonconvex polygons and polyhedra*, Comput. Mech., 56 (2015), pp. 967–981.
[32] D. Di Pietro and S. Krell, *A Hybrid High-Order method for the steady incompressible Navier–Stokes problem*, J. Sci. Comput., 74 (2018), pp. 1677–1705.
[33] D. Di Pietro and S. Lemaire, *An extension of the Crouzeix–Raviart space to general meshes with application to quasi-incompressible linear elasticity and Stokes flow*, Math. Comp., 84 (2015), pp. 1–31.
[34] D. A. Di Pietro, A. Ern, A. Linke, and F. Schieweck, *A discontinuous skeletal method for the viscosity-dependent Stokes problem*, Comput. Methods Appl. Mech. Engrg., 306 (2016), pp. 175–195.
[35] A. L. Gain, G. H. Paulino, S. Leonardo, and I. Menezes, *Topology optimization using polytopes*, Comput. Methods Appl. Mech. Engrg., 293 (2015), pp. 411–430.
[36] A. L. Gain, C. Talischi, and G. H. Paulino, *On the virtual element method for three-dimensional linear elasticity problems on arbitrary polyhedral meshes*, Comput. Methods Appl. Mech. Engrg., 282 (2014), pp. 132–160.
[37] F. Gardini and G. Vacca, *Virtual element method for second order elliptic eigenvalue problems*, IMA J. Numer. Anal., (2017), https://doi.org/10.1093/imanum/drx063.
[38] V. Girault and P.-A. Raviart, *Finite Element Methods for Navier-Stokes Equations. Theory and Algorithms*, Springer Ser. Comput. Math. 5, Springer-Verlag, Berlin, 1986.
[39] V. John, A. Linke, C. Merdon, M. Neilan, and L. G. Rebholz, *On the divergence constraint in mixed finite element methods for incompressible flows*, SIAM Rev., 59 (2017), pp. 492–544.
[40] A. Linke and C. Merdon, *On velocity errors due to irrotational forces in the Navier-Stokes momentum balance*, J. Comput. Phys., 313 (2016), pp. 654–661.
[41] Y. Maday and A. Quarteroni, *Approximation of Burgers' equation by pseudospectral methods*, RAIRO Anal. Numér., 16 (1982), pp. 375–404.
[42] G. Manzini, A. Russo, and N. Sukumar, *New perspectives on polygonal and polyhedral finite element methods*, Math. Models Methods Appl. Sci., 24 (2014), pp. 1665–1699.
[43] D. Mora, G. Rivera, and R. Rodríguez, *A virtual element method for the Steklov eigenvalue problem*, Math. Models Methods Appl. Sci., 25 (2015), pp. 1421–1445.
[44] S. E. Mousavi and N. Sukumar, *Numerical integration of polynomials and discontinuous functions on irregular convex polygons and polyhedrons*, Comput. Mech., 47 (2011), pp. 535–554.

[45] A. Ortiz-Bernardin, A. Russo, and N. Sukumar, *Consistent and stable meshfree Galerkin methods using the virtual element decomposition*, Internat. J. Numer. Methods Engrg., 112 (2017), pp. 655–684.
[46] I. Perugia, P. Pietra, and A. Russo, *A plane wave virtual element method for the Helmholtz problem*, ESAIM Math. Model. Numer. Anal., 50 (2016), pp. 783–808.
[47] W. Qiu and K. Shi, *A superconvergent HDG method for the incompressible Navier–Stokes equations on general polyhedral meshes*, IMA J. Numer. Anal., 36 (2016), pp. 1943–1967.
[48] P. G. Saffman, *On the boundary condition at the surface of a porous medium*, Stud. Appl. Math., 50 (1971), pp. 93–101.
[49] A. Sommariva and M. Vianello, *Product Gauss cubature over polygons based on Green's integration formula*, BIT, 47 (2007), pp. 441–453.
[50] C. Talischi, G. H. Paulino, A. Pereira, and I. F. Menezes, *PolyMesher: A general-purpose mesh generator for polygonal elements written in Matlab*, Struct. Multidiscip. Optim., 45 (2012), pp. 309–328.
[51] G. Vacca, *Virtual element methods for hyperbolic problems on polygonal meshes*, Comput. Math. Appl., 74 (2017), pp. 882–898.
[52] G. Vacca, *An H^1-conforming virtual element for Darcy and Brinkman equations*, Math. Models Methods Appl. Sci., 28 (2018), pp. 159–194.
[53] P. Wriggers, W. Rust, and B. Reddy, *A virtual element method for contact*, Comput. Mech., 58 (2016), pp. 1039–1050.
[54] J. Zhao, S. Chen, and B. Zhang, *The nonconforming virtual element method for plate bending problems*, Math. Models Methods Appl. Sci., 26 (2016), pp. 1671–1687.